THE PENNSYLVANIA STATE UNIVERSITY
SCHREYER HONORS COLLEGE

DEPARTMENT OF CHEMICAL ENGINEERING

Removal of Antibiotics from Water Using Functionalized Celluloses

DAVID KENNEDY
SPRING 2021

A thesis
submitted in partial fulfillment
of the requirements
for baccalaureate degrees
in Chemical Engineering and Chemistry
with honors in Chemical Engineering

Reviewed and approved* by the following:

Amir Sheikhi
Assistant Professor of Chemical Engineering
Thesis Supervisor

Wayne Curtis
Professor of Chemical Engineering
Honors Adviser

* Electronic approvals are on file.

ABSTRACT

The continual evolution of bacteria to resist treatment with antibiotics has become a looming crisis, especially amplified by the bioconcentration of antibiotics in water sources and excess antibiotics in the serum when prescribed, each leading to off-target antibiotic resistance and a possible future where society loses its greatest tool in fighting off disease. In this work, a novel adsorbent for removing especially crucial antibiotics of last resort, mainly vancomycin, but also linezolid, was been synthesized from cellulose of two different sources: Whatman filter paper and Softwood Kraft Pulp through sequential periodate oxidation to form DAMC (dialdehyde modified cellulose) fibers followed by chlorite oxidation. The microfibrous precipitate, a previously discarded byproduct in electrosterically stabilized nanocrystalline cellulose (ENCC) synthesis was synthesized and characterized through light microscopy and carboxylate content by conductometric titration (2.26 mmol/g filter paper and 4.22 mmol/g softwood Kraft pulp) before being used for removal experimentation. The carboxylated cellulose microfibers were shown to effectively bind and precipitate vancomycin from solution, with the Whatman Filter Paper product proving to be more effective than Softwood Kraft Pulp with a removal capacity of 2116 mg/g, which is nearly triple the highest reported removal capacity for any other adsorbent in the literature, compared to a still stellar 782 mg/g for the Softwood Kraft Pulp fibers. The mechanism of action was shown to be through electrostatic interaction, as proven by varying pH to show that removal only proceeded effectively in the pH range where vancomycin was protonated while the carboxylates of the filter paper microfibers were deprotonated, and the aldehyde containing fibers that get carboxylated in the microfibrous precipitate synthesis showed no removal. The presence of competing Na^{+} and Ca^{2+} cations were

found to decrease removal ability incrementally with their increased concentrations and upon modelling to the Langmuir fit, it was shown that this adsorption behavior fits very well to the Langmuir monolayer isotherm. Finally, the filter paper microfibers were found to be inefficient at removing linezolid from solution, especially compared to ENCC, though neither anionic cellulosic derivative was very successful at removing the uncharged linezolid.

TABLE OF CONTENTS

LIST OF FIGURES

LIST OF TABLES

ACKNOWLEDGEMENTS

I would first like to thank the incredibly supportive and patient colleagues in the Sheikhi Lab at Penn State. First and foremost, Dr. Amir Sheikhi, for taking me on as his first undergraduate student at Penn State and constantly supporting my research endeavors while never running out of creative ideas for me to pursue in the lab. His trust in me while constantly helping me to push the boundaries of the field has been a formative part of my college experience. I'd also like to thank the graduate and undergraduate researchers in the Sheikhi Lab, especially Mica Pitcher and Joy Muthami. Both Mica and Joy have been incredibly supportive and patient with me, while teaching me more than they know; they consistently went out of their ways to help me when truly did not have to, for which I am incredibly grateful. Much of the basis of this work came from techniques I learned from Mica and Joy, and without their help from material preparation to aiding with data analysis, this thesis would not have been possible.

Next, I would like to thank the entire Chemical Engineering Department at Penn State. Throughout my four years here, this department has allowed me to learn the foundational principles of chemical engineering while giving me unmatched opportunities to apply my education in the lab. I'd like to thank Dr. Curtis and his graduate students especially for taking me on as a freshman and allowing me to develop my research skills early on which laid the groundwork for success in Dr. Sheikhi's lab the last two years. I am grateful that my education from the Penn State Chemical Engineering Department afforded me the flexibility and opportunity to further apply my classroom education and pursue a co-op at Vertex Pharmaceuticals spring 2020, which is an opportunity that will likely shape my career. I would finally like to thank Dr. Stephanie Velegol, who will be serving as my Faculty Marshall at

graduation, for being among the most passionate educators I've ever had; from my very first chemical engineering class, Material Balances freshman year, through Chemical Engineering in the Environment senior year, her education has both taught me the fundamentals of chemical engineering, but also guided me in choosing a future career path.

As I think back on the people who most shaped who I have become, I would be remiss to not mention my high school physics teacher, Mr. Dan Cipolla. His passion as an educator and drive to see his students succeed are a large part of me pursuing STEM, and the work I was able to do with him leading the Engineering Club in high school helped guide me to where I am today.

Furthermore, the PSU Club Cross Country team has been one of the few constants throughout the last four years of my life, even in this reduced form during COVID. Knowing every day, that no matter how stressed or worn down I was, I'd be able to see fifty-plus smiling faces of my friends at 4:30 at Rec Hall was exactly what I needed to get through college. Singing the Alma Matter with nearly a hundred of my teammates after winning a National Championship in 2019 will forever be one of my most cherished memories, and this team has truly shaped my college experience. It has even given me six phenomenal roommates that have supported me endlessly and notably made the last two years very memorable, so thank you to Aidan, Aidan, David, Mike, Steve, and Nate.

Finally, I want to express my gratitude for the people in my life who have supported me from the very start, my family. I've found that growing up in a family that encourages curiosity, intellectual pursuits, and places so much value on education is a very special thing; their guidance throughout my life has shaped who I have become, and I will be forever grateful for their incessant guidance and support.

Introduction

The development of antibiotic resistance by infectious bacteria and fungi presents a critical problem for the next generation of scientists, both in maintaining the efficacy of current drugs to combat disease, and also in removing the excess antibiotics from the water we drink to minimize our exposure. As antibiotics are administered and subsequently bioconcentrated in water sources, microbes respond by developing antibiotic resistance through mutation or horizontal gene transfer.[1] At the same time, discovery of new antibiotics has slowed sharply as a number of commercial incentives to development have dwindled. At the same time, the most obvious mechanisms of action against bacteria have all been pursued and discovered leaving it far more difficult to develop a new antibiotic now than it was in 1960. As a result, the same antibiotics are being prescribed and resistance to those antibiotics is become a rampant problem as selective pressure is put onto bacteria and fungi to evolve resistance to that set of antibiotics.

1. Antibiotic Resistance Background

Importance of Antibiotics and Growing Concerns

Alexander Fleming's isolation of penicillin from a fungus of the *Penicillium* genus is considered among the greatest medical discoveries in human history, and has been considered responsible for preventing hundreds of millions of deaths from infection since its large-scale development began during World War II.[2] While culturing his

staphylococcal bacteria strain, Fleming noticed mold contamination. Just as he was ready to discard the petri dish, he noticed that no staphylococci were able to grow surrounding the mold.[3] It was immediately clear the fungus was emitting some chemical that prevented the growth of the bacteria, and upon its isolation and subsequent scale-up, this chemical became the life-saving compound we now appreciate as penicillin.

In the decades following Fleming's discovery, his workflow was imitated by scientists across the globe with thousands of other fungal, bacterial, and plant strains screened against common bacterial cultures to isolate any naturally occurring antibacterial compounds.[4] The 1950s and 1960s became the "Golden Age" of antibiotic discovery with at least half of those presently used being isolated during this period, as can be seen in the timeline in **Figure 1.** At least eight new classes of antibiotics were discovered during this period, each with a different mechanism. Each new antibiotic targeted different parts of a bacterial cell, meaning resistance in development in one type would usually not extend to other types.[5] These antibiotics radically changed the scene of global healthcare; for the first time, widespread infections were treatable and preventable. For the time being, antibiotics were abundantly available and still novel enough to be incredibly effective as little resistance had been developed. However, scientists rapidly exhausted the easily accessible antibacterial sources and by the 1990s, development of new

classes had stagnated completely[6].

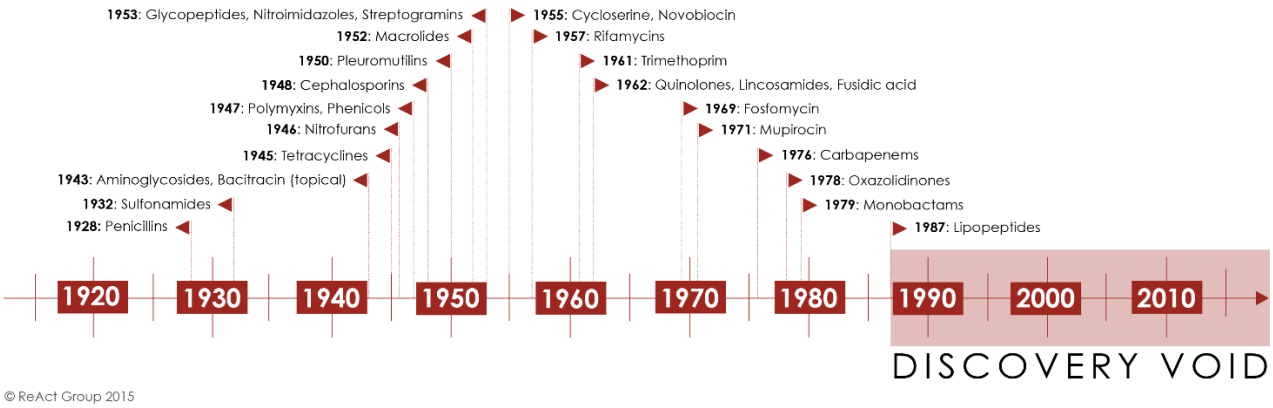

Figure 1: A Timeline of the Discovery of New Classes of Antibiotics. Notably, development of new mechanisms has stagnated for the last three decades.[6]

As hospitals continued to treat, and in some cases, over-prescribe, patients with the limited scope of antibiotics available, the bacterial and fungal cells those antibiotics treat gain exposure to the antibiotic. Selective pressure is thus placed on those cells to mutate to gain an antimicrobial resistance (AMR) gene; all the cells without this gene will die, while the ones that are able to mutate will continue to divide and share that gene to other cells through horizontal gene transfer.[7] With most antibiotics not being fully metabolized by the body and as a result, being excreted in urine and feces , the environmental disposition of those excreted antibiotics is of notable importance. Given that water treatment facilities are often ineffective at removing many of these drugs, the constant resupply of antibiotics into our water through prescription issuing and subsequent excretion will only continue to increase their concentration in our drinking water. Furthermore, the excess antibiotics in the body may also have devastating consequences by adapting the very cells they are meant to treat to develop antibiotic resistance. As a result, while creating a capture device for water treatment plants is valuable, an end goal of removing the drugs directly from the serum is crucial.

Current estimates place US deaths at 23,000 annually due to untreatable antibiotic resistant strains and 700,000 globally; some models have predicted the global loss to reach 10 million annually by 2050.[8] Compared to antivirals, which are used to treat viruses such as the influenza virus and prevent them from multiplying, antibiotics are effective against bacterial infections.[9] The modes through which antibiotics treat bacterial infections are numerous, and antibiotics are often classified by the way they inhibit bacterial growth or reproduction; a summary of noteworthy antibiotic classes, examples of constituent antibiotics, and their mode of action against bacteria are summarized in **Table 1.**

Table 1: Summary of notable antibiotic classes and mode of action for numerous antibiotic types

Antibiotic Class	Example Antibiotic(s)	Mode of Action
Tetracyclines	Tetracycline, doxycycline, minocycline	Interrupt bacterial protein synthesis by interfering with the binding of the 16S r-RNA on the 30S subunit to prevent binding of t-RNA.[10]
Beta-Lactams	Penicillin, Amoxicillin, Ampicillin	Cause bacterial cell lysis by mimicking the D-alanyl D-alanine region of peptide chain and prevents the proliferation of the peptidoglycan layer by preventing binding of the penicillin binding protein.[11]
Glycopeptides	Vancomycin	Prevent cell wall synthesis by binding to the D-alanyl D-alanine region of the peptidoglycan subunit to prevent penicillin binding protein attachment.[12]
Lipopeptides	Daptomycin	Disrupt the membranes of gram-positive bacteria by mimicking cationic antimicrobial peptides and inserting into the cell membrane to lead to cell death.[13]
Oxazolidinones	Linezolid	Inhibit bacterial protein biosynthesis by binding to the 23S rRNA of the 50S subunit and interacting with peptidyl-t-RNA.[14]

II. Antibiotic Resistance Development

The modes of action are important towards understanding the ways that bacteria can develop resistance to each class of antibiotic. Generally, the process for developing antibiotic resistance in infectious bacteria proceeds because of the mode of action of the antibiotic; the antibiotics each disrupt the targeted region of the bacteria, whether it be the ribosomal RNA subunits, the transcription-RNA, or penicillin binding protein. Antibiotics are clearly effective at killing bacteria through the aforementioned modes of action that often prevent crucial protein synthesis or accelerate cell lyses; however, evolution is an opposing factor that bacteria use to push back against any threatening external stimuli.[15] Excess use of antibiotics may initially kill off the pathogen as desired, but after prolonged exposure, the bacteria will begin to adapt to the resistance through the evolution of the region targeted by the antibiotic; as the selection pressure is put onto the bacteria to develop resistance, some cells will develop mutations that change the antibiotic targeted region to enable survival despite antibiotic presence.[16] This process facilitates the development of an antibiotic resistance gene and renders the antibiotic unable to continue to interrupt the proliferation of the pathogen through the aforementioned mode of actions, since the target sequence has been altered to no longer be targeted by the antibiotic. This evolution can be developed through either horizontal gene transfer, whereby the gene is transferred laterally from cell to cell, or vertical gene transfer from parent to offspring.[17] Regardless, the mutation for antibiotic resistance is coded and spread such that the antibiotic no longer affects the pathogen, and as the antibiotic resistant species gains prevalence, humans will be without their greatest tool to prevent bacterial infections.

III. Sources of the Excess Antibiotic Problem and Relevance

The topic of waste water treatment is especially relevant to the impending antibiotic resistance crisis because of the aforementioned risks of excess presence of antibiotics in contact with bacteria. When people take antibiotics, , between 10 and 90% of the ingested content is excreted as accounted for from the solid and liquid pathways, which does not even account for the excretion of metabolites such as glucuronidated, sulfated, and acetylated forms that can rapidly be transformed back into the original antibiotic.[18,19] In addition to the excretion of antibiotics being a significant contributor to presence in wastewater, this issue is compounded by the fact that between a third and a half of all antibiotic prescriptions are unnecessarily prescribed.[20] The final, significant source of excess environmental antibiotic is their use on livestock and animals to be raised as a food source in general due to the enormous benefits in meat yield, size, and overall strength of the animals. An FDA report on the purchasing habits for antibiotics in the US showed that in 2015, 70% of all antibiotics in the United States were purchased for use on animals rather than for humans.[21] The pharmaceuticals administered to animals, like humans, are often 10% metabolized, while the other 90% ends up in general water sources with minimal wastewater treatment. In fact, antibiotics tend to be metabolized to an even lesser degree in animals compared to in humans.[22] Thus, there are significant sources that contribute to the accumulation of excess antibiotics in the environment in general, largely in wastewater. As a result, wastewater treatment is critical to remove the antibiotic presence from our wastewater before the water is sent out to municipalities to be consumed and perpetuate the cycle of both exposing cells to antibiotics and largely excreting the excess back into the water system.

Presently, however, the traditional wastewater treatment process is inadequate in removing antibiotics and other non-biodegradable organic pharmaceuticals from water. Wastewater treatment plants (WWTPs) are simply not designed to remove antibiotics from water, as their purpose is largely to remove biological oxygen demand (BOD), which generally refers to oxidizable organics in the water, but since WWTPs functionally work as bioreactors to remove this BOD, any molecules the bacteria cannot oxidize will not be removed.[23] Chemical oxygen demand (COD) refers to all the possible oxidizable material in the influent, but since antibiotics, for example, are chemically oxidizable, but not oxidizable by bacteria, they constitute COD but not BOD and will remain in the treated effluent to be bioconcentrated, and part of the water influent further down the watershed.[24]

IV. Historical Trend of Antibiotic Resistance and Drugs of Last Resort

As various antibiotics are increasingly being detected at ng/L to μg/L concentrations in the influent of wastewater, yet hardly being removed during processing. At the same time, additional antibiotics are consistently being added into wastewater, the mass balance indicates a continuous increase in antibiotic concentration in municipal water. The consequences of such a perpetual increase in concentration for these drugs in wastewater are widespread and expressed as the development of antibiotic resistance while contributing to the trend of humanity losing its greatest tool in staving off the ills of bacterial infections.

While pathogens developing resistance to any antibiotic is a serious risk to society, certain antibiotics are more crucial to our fight against disease, and more importantly, preserving our future ability to fight it off. The timeline of antibiotic introduction into the healthcare system

paralleled with the first identification of antibiotic resistance for those developments is telling to how grave this situation is. Though penicillin was initially discovered in 1928 by Alexander Fleming, it was not introduced into hospitals widespread until the early 1940s and played a significant role in warding off bacterial infections in the Second World War.[25] By the 1950s, however, penicillin resistance was already such a serious problem in hospitals that any improvements in survival rates from infection gained by the discovery of antibiotics had begun to be threatened.[26] Before antibiotics, deaths from infections of *Staphylococcus aureus*, *Streptococcus pneumoniae*, and *Mycobacterium tuberculosis* were rampant, and *Staphylococcus aureus* for example posted an 80% mortality rate among the people infected with the bacteria.[27,28] The timeline in **Figure 2** illustrates the rapid ability of bacterial infections to develop resistance following widespread use of the antibiotic, with resistance often following the introduction by between one and two decades.[29] Startlingly though, the development of new antibiotics, especially antibiotics that work through new modes of action, has virtually ceased since the 1980s, and so as the old antibiotics lose their potency, they are not actively being replaced with new functioning drugs, and so a significant effort has been made to protect the remaining working antibiotics.

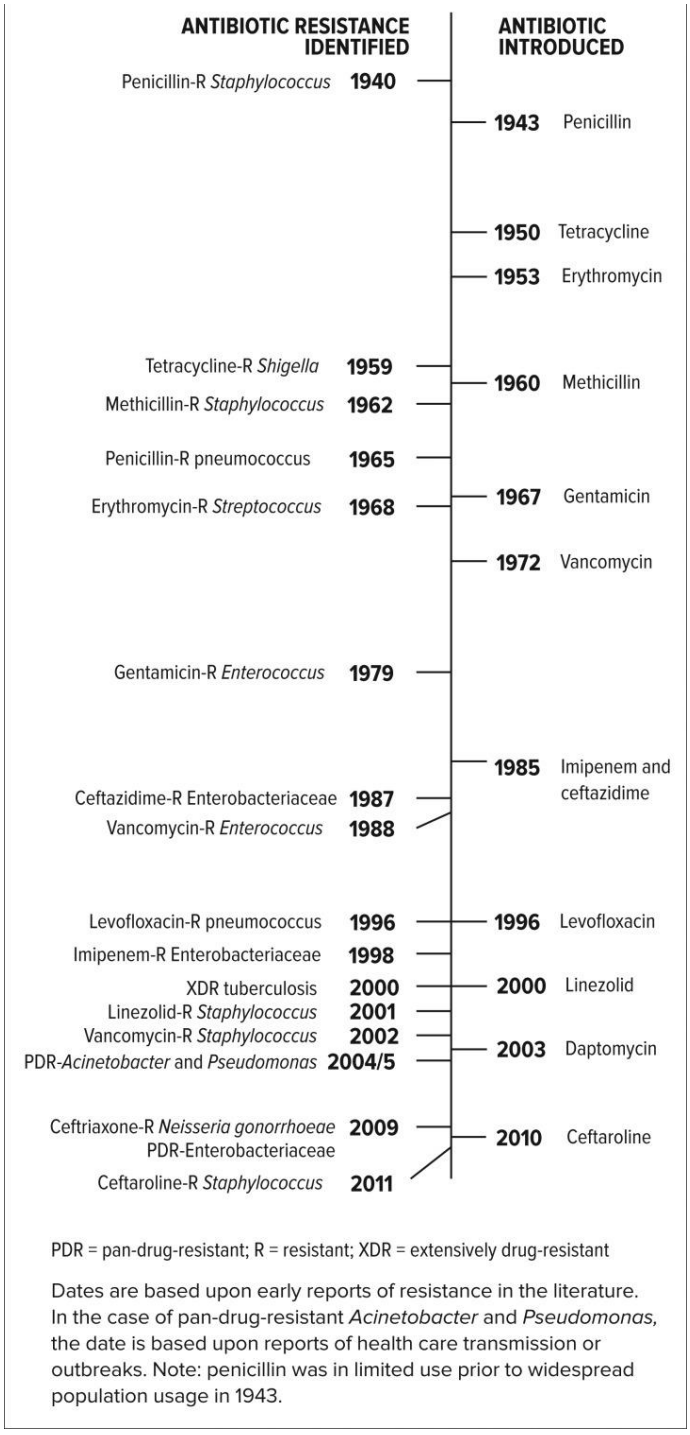

Figure 2: Timeline of Antibiotic Introduction and Identification of Antibiotic Resistance[29]

Some of the most common types of resistant bacteria seen in hospitals are Penicillin-resistant *Streptococcus pneumonia* (PRSP) and Methicillin-Resistant *Staphylococcus aureus*

(MRSA) among others.[30] MRSA, representing the resistance to treatment of the *Staphylococcus aureus* strain with an 80% mortality rate without antibiotics is considered one of the most pressing challenges in this crisis, and it is becoming exceedingly common. As a result, numerous other antibacterials that are newer, and thus have lower rates of resistance as seen in hospitals around the world, have been set aside by the scientific and healthcare community as antibiotics of "last resort" or "anti-MRSA" pharmaceuticals, with several options of antibiotics issued for MRSA strains; several examples of target organs and the reliable antibiotic are listed in **Table 2**.[31]

Table 2: Summary of Anti-MRSA Pharmaceuticals. Vancomycin is noted in each infectious focus[31]

Target Organ of Infection	Anti-MRSA Antibiotic Choices
Soft tissue/skin	Vancomycin Daptomycin Linezolid,
Lungs	Vancomycin Linezolid
Blood	Vancomycin Daptomycin

As described in **Table 2**, the most prevalent antibiotics issued in hospitals as "last-resort" for resistant strains are linezolid, vancomycin, and daptomycin; therefore, this work will focus on these antibiotics. These choice drugs, whose structures appear in **Figure 3**, must be protected at all costs especially since antibiotic innovation has slowed, and these truly represent the last resort for patients against the constantly evolving pathogens.[32]

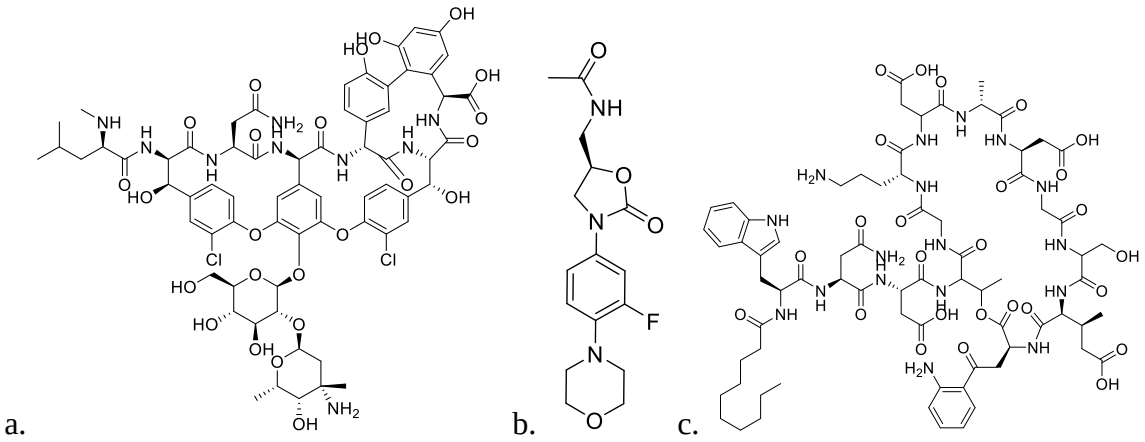

Figure 3: Structures of Key MRSA Last-resort Antibiotics: a. vancomycin, b. linezolid, c. daptomycin

Concerningly, incidence of multi-drug resistant pathogens is on the rise. Despite vancomycin having been set aside to be used sparingly as a drug of last resort, there have been rising reports of levels of vancomycin resistance among *Staphylococcus aureus*, falling into the category of vancomycin intermediate *S. aureus* (VISA) with resistance up to moderate doses of a minimum inhibitory concentration of up to 8 μg/mL, which used to readily treat the infection.[33] Furthermore, even more concerning are the reports of completely resistant strains of *S. aureus* labeled VRSA (vancomycin resistant *S. aureus*) which survive even when being treated with vancomycin doses upwards of 16 μg/mL.[33] A 2016 study from burn victims in Bangladesh hospitals showed that upwards of two-thirds of *Staphylococcus aureus* strains isolated showed methicillin resistance (MRSA) with just over 50% of those strains also showing resistance to vancomycin.[34] While US resistance rates have trailed those of Bangladesh, this trend is still alarming.[35]

Other drugs of last resort for methicillin resistant *Staphylococcus aureus* follow this similar trend; resistance is emerging, and though newer antibiotics may have lower rates, the situation is constantly worsening as pathogens evolve. Linezolid, for example, was noted as the

drug of choice for MRSA strains in the lungs and skin or soft tissue.[31] Linezolid remains incredibly effective at treating all gram-positive pathogens, and over 90% of gram-positive strains are inhibited at levels below 4 μg/mL. Yet, 1% of *S. aureus* strains have been shown to be fully resistant to linezolid, which is encouragingly low, but concerning considering linezolid was introduced in 2000, far more recently than daptomycin and vancomycin.[36]

Like linezolid, daptomycin, which was introduced in 2003, has lower rates of antibiotic resistance in *Staphylococcus aureus,* but these rates are still high enough to be alarming. Between 0.1% and 0.3% of methicillin resistant *S. aureus* strains showed daptomycin resistance, which is even lower than both linezolid and vancomycin.[37] The low rate of resistance is a good sign for applicability of both daptomycin and linezolid as the crucial remaining option. However, considering the critical bulwark these medicines provide in fighting off bacterial pathogens, maintaining these low resistance percentages is critical. Largely, this goal can be achieved by limiting bacteria's exposure to these antibiotics in unnecessary situations, which can first occur by prescribing lower doses of vancomycin, linezolid, and daptomycin, but also requires initiatives to lower the contact of these antibiotics with the pathogens, largely in the water we drink. Mid-Atlantic water has increasing levels of antibiotics across the board, and though the literature is sparse on levels of vancomycin and daptomycin, they are expected to be even higher than the 28 ng/mL for linezolid.[38] Accompanying this antibiotic presence, pathogen strains resistant to these antibiotics, especially vancomycin, are also being found in wastewater.[39]

Wastewater treatment is currently lacking in preventing the accumulation of antibiotics in water sources, and so this work focuses on developing novel adsorbents for the precipitation and removal of these substances from wastewater.

2. Celluloses Background

Cellulose is the most abundant biopolymer in the world, and as such a widely available material, its development as a feedstock for useful applications including as a fuel source or adsorbent provides a green source with many advantageous properties. Its abundance is a chief reason why cellulose makes for such a good polymer backbone to be functionalized for value-added applications; it is the most abundant organic molecule on earth, and further can be produced on the scale of 100 billion tonnes per year.[40] Due to its renewability and being sourced from plants, cellulose is further a great adsorbent given the impending climate situation. Further modifications of this abundant biopolymer enable researchers to optimize its physical properties including charge, strength, and crystallinity and produce robust adsorbents for any target compound.

Meanwhile, the structure of cellulose itself, with a primary hydroxyl and two vicinal diols per subunit enable such chemical functionalization, as shown in **Figure 4**. The cellulose polymer is assembled from repeating β-1,4-linked glucopyranose units that alternate in their orientation by 180°; the carbons are numbered on each monomer by placing the anomeric carbon as number 1 and then tracing the ring away from the oxygen while counting up.[41] The repeated structure of cellulose enables targeted medications to implement a wide variety of chemical groups.

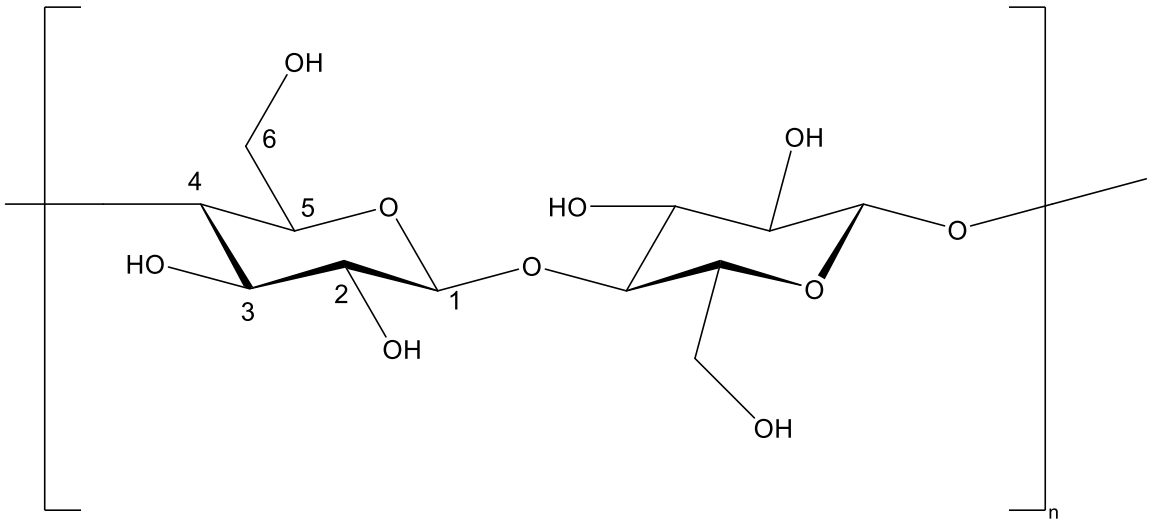

Figure 4: Cellulose Structure with Carbons Numbered

The degree of crystallinity of cellulose is also an important factor in determining its properties and also permitting different chemical reactions to attack portions of the polymer while shielding others. While the source of the cellulose impacts the degree of crystallinity, cellulose is in general composed of alternating crystalline and amorphous regions; while the crystalline regions are ordered and strongly organized due to hydrogen bonds and other inter and intra-molecular forces, the amorphous regions are exactly the opposite: disordered and lacking shape.[42] Due to the rigidity of the crystalline regions, molecular access to the reactive sites is more constrained, and chemical modification targets the amorphous regions of cellulose selectively. Reacting the cellulose enables the amorphous regions to be selectively reacted while the crystalline regions of cellulose remain intact.[43] A very common and useful application of this selectivity is the hydrolysis of the amorphous regions by a strong acid, such as sulfuric acid, to disintegrate the amorphous regions and yield cellulose nanocrystals, and while nanocrystalline cellulose of this type is interesting for its crystallinity, it has the significant downsides of low functionalization ability and colloidal stability.[44,45,46]

Instead, different chemistries can be applied to the cellulose polymer to maintain functionalization while remaining stable in solution. A common reaction to achieve functionalization of cellulose is periodate oxidation, which still targets the amorphous regions and enables the cellulose to become solubilized, but it leaves "hairs" of the protruding functionalities in the process.[47] By grinding up the cellulose source to increase its reactant surface area and stirring in sodium periodate, the vicinal diols in the β-1,4-linked glucopyranose units are converted to aldehydes as the C2-C3 bond is cleaved.[46] The product of this periodate oxidation is referred to as dissolved dialdehyde modified cellulose; these aldehydes are then reactive for widespread other chemical reactions that can then impart different functionalities on carbon 2 and carbon 3.

While fibers of the cellulose polymer span the micro to macro scale, with dimensions of about a few mm in length by up to 50 μm, accessing nano scale cellulose has tremendous advantages in advanced applications.[48] For water treatment, for example, nanocellulose is advantageous because it can be modified chemically while retaining a high surface area to volume ratio. The charge content that can be accessed by functionalized nanocellulose crystals is also very high, and can reach upwards of 6 mmol of carboxylate per gram of material, which enables high levels of electrostatic interactions that cannot be accessed by other adsorbents.[49]As a result, in the process of imparting functional groups, it is advantageous to transform the cellulose into nanocrystalline forms, which is seen in the conversion of dialdehyde modified cellulose to various hairy cellulose nanocrystals.

A summary of the chemistry that can be applied to dissolve dialdehyde modified cellulose and subsequent derivatives appears in **Figure 5**; each functionalization belongs to the hairy cellulose nanocrystalloids class of nanomaterials due to the solubilized amorphous regions

and protruding functionalities mimicking hairs. After periodate oxidation to produce dissolved dialdehyde modified cellulose (DAMC), to maintain the neutrality, but ensure crystallinity, the DAMC can be stirred while heating at 80°C in an oil bath for 6 hours to yield sterically stabilized nanocrystalline cellulose (SNCC); experimentation by Yang et al. at McGill University showed the degree of polymerization was reduced to 532 after 6 hours at 80°C and even further to 21 after 6 hours at 90°C from cotton's original degree of polymerization of approximately 10,000.[50,51]

In order to take advantage of the functionalization of cellulose nanocrystals using electrostatic interactions, a negative charge can be imparted onto the DAMC. Following sodium periodate oxidation, further oxidation using sodium chlorite enables the conversion of the aldehydes on carbons 2 and 3 into carboxylic acid groups to yield a material called electro sterically stabilized nanocrystalline cellulose or ENCC. The Pinnick Oxidation generally described the conversion of an aldehyde to a carboxylic acid using chlorite, as occurs to the DAMC in this reaction.[52] In addition to ENCC, a byproduct forms from the dissolving of the

amorphous regions known as dicarboxylated cellulose, or DCC.

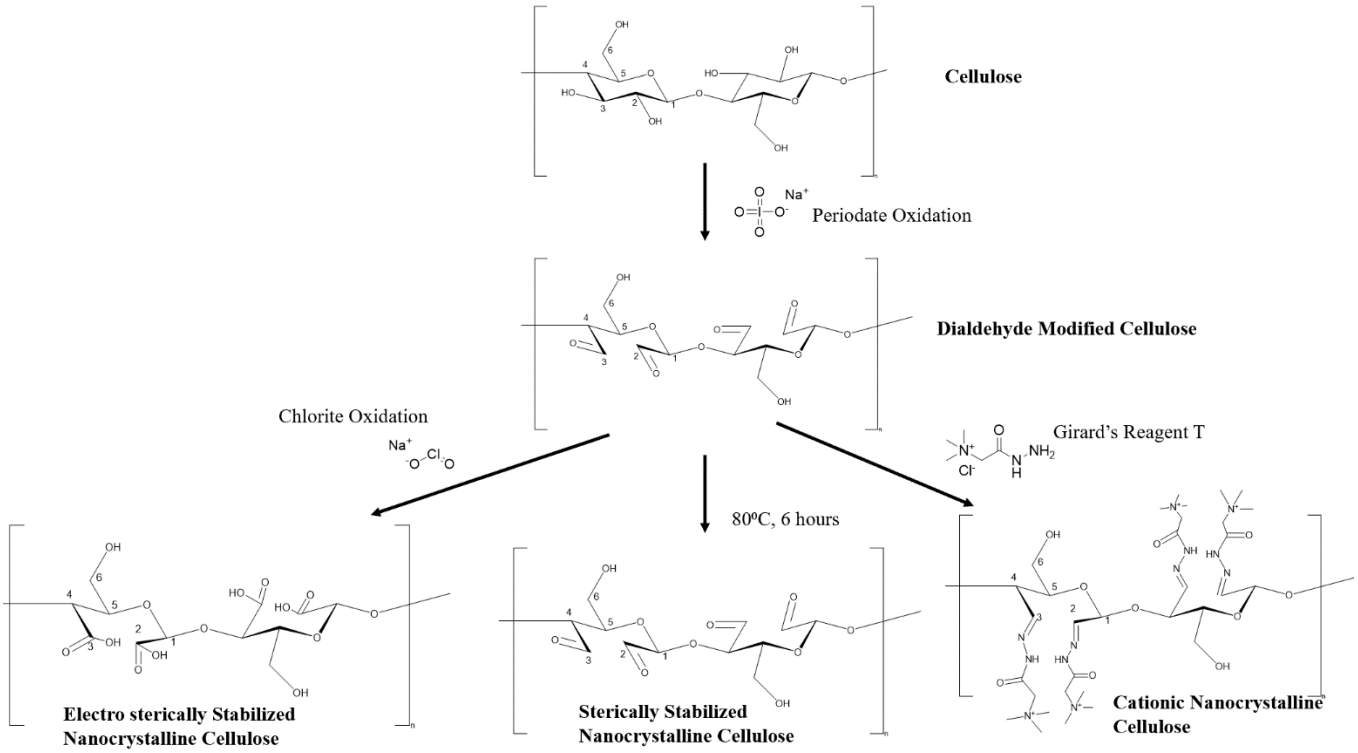

Figure 5: Hairy Nanocellulose Crystalloid Derivatives and Applicable Chemical Reactions

I. Hairy Nanocellulose Crystalloids

The existence of protruding "hairs" off of the crystalline backbone makes hairy nanocellulose crystalloids particularly interesting as adsorbents.[47] They can maintain high functionality content, and notably extend these functionalities off the backbone of the biopolymer to interact with other functionalities in the surrounding media. For wastewater treatment and adsorption applications, this is a desired property because the functional group interactions drive the toxin or other pollutant to bind and be removed from solution; increasing the potential surface area and space overall for this interaction increases the ability of the material to remove the pollutant from water samples. Another important function of the

adsorbent is its ability to separate from the solution itself; binding the pollutant is one problem that can be solved by forming the desired interactions, but an entirely different problem is the actual removal of that bound complex from solution, and this issue presents challenges, especially for low concentrations of pollutants since these low concentrations are much more difficult to precipitate.[53,54]

The three main classes of hairy nanocelluloses are arranged according to their charges, as indicated in **Figure 5**. These classes are the neutrally charged sterically stabilized nanocrystalline cellulose which contains aldehyde groups, the negatively charged electrosterically stabilized nanocrystalline cellulose with its carboxylic acid functionalities, and the cationic nanocrystalline cellulose with its positively charged quaternary ammonium functionalities. To synthesize each of these a common intermediate is used: dialdehyde modified cellulose.[55] The presence of aldehyde groups formed by cleaving the vicinal diols in cellulose enables functionalization due to the reactivity of aldehydes. While the aforementioned treatment of DAMC with elevated temperature (80°C) can yield neutrally charged aldehyde modified sterically stabilized nanocrystalline cellulose, to impart positive charge, a Schiff-Base reaction can be utilized. The Schiff-Base reaction generally links primary amines and aldehydes or ketones, creating an imine bond between the carbon and the nitrogen of the amine.[56] For the application of functionalizing nanocelluloses, this reaction could be used to explore a broad chemical functional space by modifying the aldehydes of DAMC with of the abundant commercially available amines, but in this case, Girard's Reagent T, whose structure appears in **Figure 6** is the amine used to create cationic nanocrystalline cellulose.

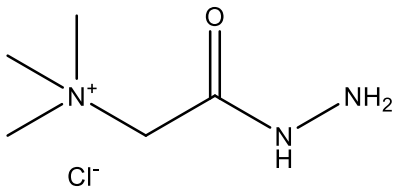

Figure 6: Girard's Reagent T Structure

These CNCCs (cation nanocrystalline celluloses) have been extensively applied in the literature due to their advantageous properties of moderate charge content for a bio-based material while remaining 67% crystalline.[57] CNCCs have been used for removal of anionic toxins and pollutants in water such as dyes and antibiotics, as a retention additive in paper processing, and as a flocculant for microalgae harvesting.[58,59,60] This material has potential for removal of anionic contaminants especially, due to the electrostatic interaction.

Of the hairy nanocellulose crystalloids, the most relevant to this work is the negatively charged electro sterically charged nanocrystalline celluloses, ENCC. Vancomycin, which is among the most common antibiotics of last resort for anti-MRSA and other infections that have developed microbial resistance, is positively charged as seen in its protonation state at physiological pH in **Figure 7.**

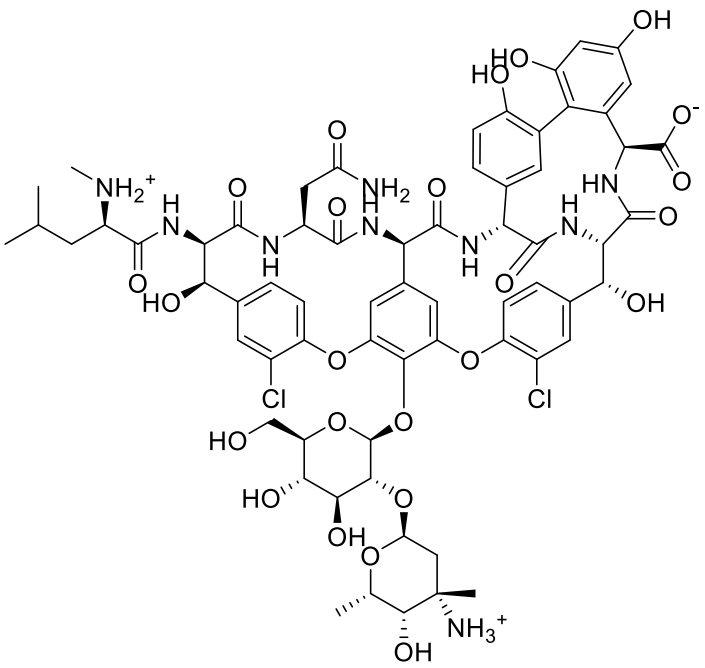

Figure 7: Protonation State of Vancomycin at Physiological pH (pH 7). Vancomycin has a net +1 charge

At a physiological pH of between 6.5 and 7, the primary amine and secondary amine will each be protonated while the carboxylic acid, with a pKa of approximately 5, will be deprotonated, yielding a net charge of +1 for vancomycin. Thus, vancomycin is best removed by an anionic adsorbent. Due to their high charge content compared to other adsorbents, especially compared to other functionalized biopolymers, above 6 mmol of negatively charged carboxylate per gram of material, ENCC and other anionic celluloses are ideal for removal of vancomycin. As such, the synthesis and products of ENCC synthesis are of notable interest. ENCC has been used extensively for the removal of positively charged contaminants from water such as cationic dyes such as methylene blue or harmful metal ions such as copper (II).[61,62]

The aforementioned process of synthesizing ENCC using periodate oxidation to cleave the vicinal diols of celluloses into aldehydes to form DAMC followed by chlorite oxidation to oxidize the aldehydes into carboxylic acids is a well-documented synthesis in the literature, but

in addition to ENCC, it also forms byproducts. These byproducts include a microfibrous precipitate section that precipitates out before ethanol addition, ENCC, and DCC.

While ENCC is advantageous for being the most water soluble and having the highest charge content, this reaction additionally forms a heavier and a lighter product, both of which are carboxylated, but each having unique and applicable properties. The precipitation experiment shown in **Figure 8** shows the distinct fractions for the two carboxylated cellulose disintegrated materials: ENCC and DCC (dicarboxylated cellulose), whereby ethanol was used as a cosolvent to incrementally precipitate and purify the different materials since it would force the more polar material to crash out of solution sooner due to addition of less polar ethanol to the water solution.

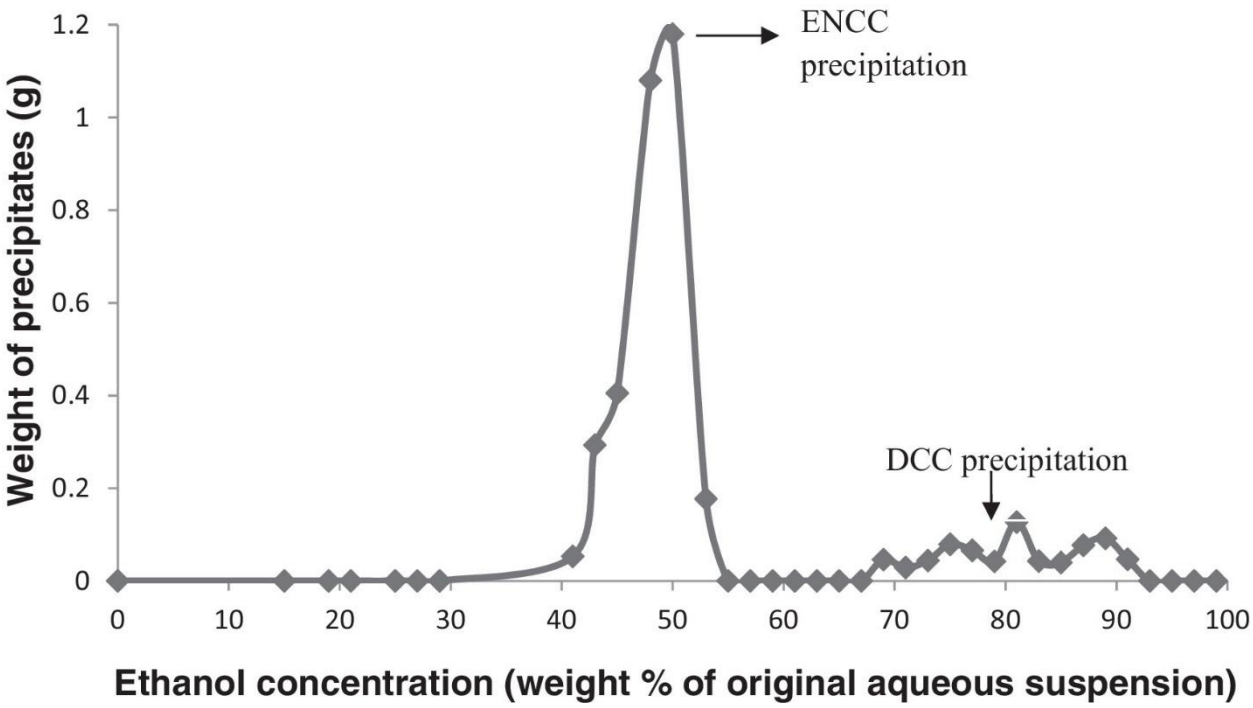

Figure 8: Precipitation for Separation of ENCC and DCC[63]

While the precipitation graph in **Figure 8** neglected the first fraction of material that precipitates before any ethanol addition since it was not relevant to their study, this material has been documented as a byproduct in other literature sources for the synthesis of ENCC.[64] This

first fraction is unique in containing phase separated microfibers; this microfibrous precipitate is charged between 2.2 and 4.5 mmol/gram of carboxylate with yields of 20-40% varying by cellulose source as evidenced by our research and confirmed by the initial studies of Yang et al.[64] ENCC, being the second fraction has been the most studied, and contains upwards of 6 mmol/g carboxylate, with a hydrodynamic diameter of approximately 70 nm on average.[64] Finally, the last fraction of the precipitation containing DCC, or 2,3 dicarboxylate cellulose which is smaller than ENCC, with a hydrodynamic diameter on the order of 50 nm, and contains the disintegrated hairs with higher charge content of 6.95 mmol/g.[64]

II. Limitations of ENCC for Contaminant Removal

The major limitation of ENCC is that, while effective at removing contaminants from water at high concentrations (above 4 mg/mL initial concentration), it fails to achieve low concentration removal effectively, as evidenced in the low removal capacity of methylene blue dye at low concentrations.[62] This phenomenon is due to the size and high charge content of ENCC; because it is so charged, at low concentrations, the ENCC particles do not precipitate from solution because the charge is enough to keep them solvated completely as the molecules are small enough to stay in solution. While the ENCC is interacting with the contaminants in solution at low concentration, the low concentration of the contaminant-ENCC complex is not enough to aggregate enough to crash out. As such, even though binding is occurring, removal of the contaminant is problematic because it remains in solution; therefore, whether it is on a small scale or a large scale in flocculation within wastewater treatment, ENCC is not an effective adsorbent for the trace quantities of contaminants. For the intended application of removal of

excess off-target antibiotics from the bloodstream or for wastewater treatment, where the concentrations of contaminants are far lower than ENCC's limitation, another material is required. The levels of antibiotics in the blood, such as vancomycin as the relevant example, are indicated by the trough level or low level to be achieved before the next dose of approximately 15 μg/mL with the upper bound as the reference range maximum for life threatening infections of 40 μg/mL.[65,66] Similarly, wastewater has been shown to contain concerning levels of vancomycin for the development of antibiotic resistance, but the concentration on the order of 0.0032 μg/mL is a serious challenge.[67] The main hurdle to achieve removal at lower concentrations is to enable precipitation and removal; the binding mode of action is known to be effective regardless of concentration due to the electrostatic interaction. As a result, using a carboxylated material that is already phase separated due to larger sized fibers is the desired alternative. The microfibrous precipitate of ENCC synthesis is an ideal low-cost and green alternative for contaminant removal at low concentration due to its ability to precipitate and be centrifugated rather than requiring a high contaminant binding effect to take it out of solution. Thus, this work will investigate the applications of microfibrous precipitate for antibiotic removal.

III. Cellulose Source Types

While the chemistry for cellulose conversion to microfibrous precipitate, electro sterically stabilized nanocrystalline cellulose, and dicarboxylated cellulose is well-studied and uniform, the cellulose source is very important in determining the final properties of the adsorbent material. Cellulose content is a primary metric; these cellulose sources are

predominantly made up of cellulose, but vary in their content of other compounds, largely hemicellulose. Hemicellulose is a generic name for a wide range of heteropolymers present in plant cells, made up of varying carbohydrate monomer units such as xylose, mannose, rhamnose, and galactose, with the main difference between hemicellulose and cellulose being that cellulose is a far longer polymer chain with a degree of polymerization above 10,000, while hemicellulose is on the range of 1,000 sugar subunits.[68] Higher content of hemicellulose thus, is expected to disintegrate into small particles that will precipitate less. Whatman Filter Paper, for example, is among the purest cellulose sources as it contains a minimum of 98% cotton derived α-cellulose.[69] Wood pulps, however, tend to have lower cellulose content, with hemicellulose as the bulk of the remainder; Softwood Kraft pulp, which is an extensively studied type that will be trialed in this work is 88% cellulose with the remaining 12% being hemicellulose. While the relationship between source is still unclear, the antibiotic removal abilities of the microfibrous precipitate from Softwood Kraft Pulp and Whatman Filter Paper will be compared in this work.

3. Experimentation

I. Synthesis of Cellulose Microfibrous Precipitates

To synthesize the microfibers necessary for antibiotic removal, DAMC first had to be made through periodate oxidation of cellulose which could then be exposed to chlorite oxidation for the formation of the microfibrous precipitate, ENCC, and DCC.

Filter Paper Microfibrous Precipitate

To a beaker of MilliQ water (65 mL), sodium chloride (NaCl, 3.79 g) and sodium meta-periodate ($NaIO_4$, 1.32 g) were added and stirred until dissolved. To this solution, thinly ground filter paper (1.0 g) was slowly added and allowed to react while stirring at room temperature for 42 hours. After 42 hours, ethylene glycol (1 mL) was added to quench the periodate. The filter paper dialdehyde modified cellulose was purified by extraction with MilliQ water (3 x 500 mL) filtering off using vacuum filtration each time and resuspending the solution in a fresh 500 mL of water while stirring for 30 minutes. The aldehyde content of the filter paper DAMC was characterized through conductometric titration as 5.28 mmol/g.

To a solution of sodium chlorite ($NaClO_2$, 0.8542 g) in MilliQ water (50 mL), the DAMC was slowly added while stirring. Hydrogen peroxide (H_2O_2, 0.8478 mL) was added dropwise to the reaction over 30 minutes while monitoring the pH. Sodium hydroxide (0.5 M) was added dropwise to the yellow mixture to maintain a pH of 5 while stirring for 12 hours. The now clear solution was then centrifuged for 13 minutes on at 15,000 g (12,000 rpm) to afford the **Filter Paper Microfibrous Precipitate** (632 mg, 63.2% yield) as a white clumpy fibrous material, which was redissolved to a concentration of 8.1 mg/mL. The microfibrous precipitate was

characterized through carboxylate content conductometric titration to yield 2.26 mmol/g of carboxylate.

Softwood Kraft Pulp Microfibrous Precipitate

MilliQ water (65 mL), sodium chloride (NaCl, 3.79 g) and sodium meta-periodate ($NaIO_4$, 1.32 g) were added to a beaker and stirred until dissolved. Thinly ground Softwood Kraft Pulp (1.0 g) was slowly added to this solution and allowed to react while stirring at room temperature for 42 hours. After 42 hours, ethylene glycol (1 mL) was added to quench the periodate. The Softwood Kraft Pulp dialdehyde modified cellulose was purified by extraction with MilliQ water (3 x 500 mL) filtering off using vacuum filtration each time and resuspending the solution in a fresh 500 mL of water while stirring for 30 minutes. The aldehyde content of the DAMC was characterized through conductometric titration as 8.82 mmol/g.

Sodium chlorite ($NaClO_2$, 0.8542 g) was dissolved in MilliQ water (50 mL), the DAMC was slowly added while stirring. Hydrogen peroxide (H_2O_2, 0.8478 mL) was added dropwise to the reaction over 30 minutes while monitoring the pH. Sodium hydroxide (0.5 M) was added dropwise to the yellow mixture to maintain a pH of 5 while stirring for 12 hours. The now clear solution was then centrifuged for 13 minutes on at 15,000 g (12,000 rpm) to afford the **Softwood Kraft Pulp Microfibrous Precipitate** (414 mg, 41.4% yield) as a white clumpy material, which was redissolved in MilliQ water to a concentration of 4.3 mg/mL. The microfibrous precipitate was characterized through carboxylate content conductometric titration to yield 4.22 mmol/g of carboxylate.

II. Conductometric Titration for Carboxylate Content Analysis

The determination of carboxylate content in a cellulose sample proceeds through the use of conductometric titration, which determines the amount of carboxylate present by measuring the strength of the weak acid region. As outlined in Ullmann's Encyclopedia of Industrial Chemistry, first, to a known amount of the sample was added 2 mL of 20 mM NaCl solution in 140 mL milli-Q water.[70] After setting the pH to 3.2 using 0.1 M HCl, the conductivity (mS/cm) was recorder as 10 mM NaOH was added slowly to the solution up to a basic pH of 11 using a conductometric titrator, as seen in **Figure 9.**

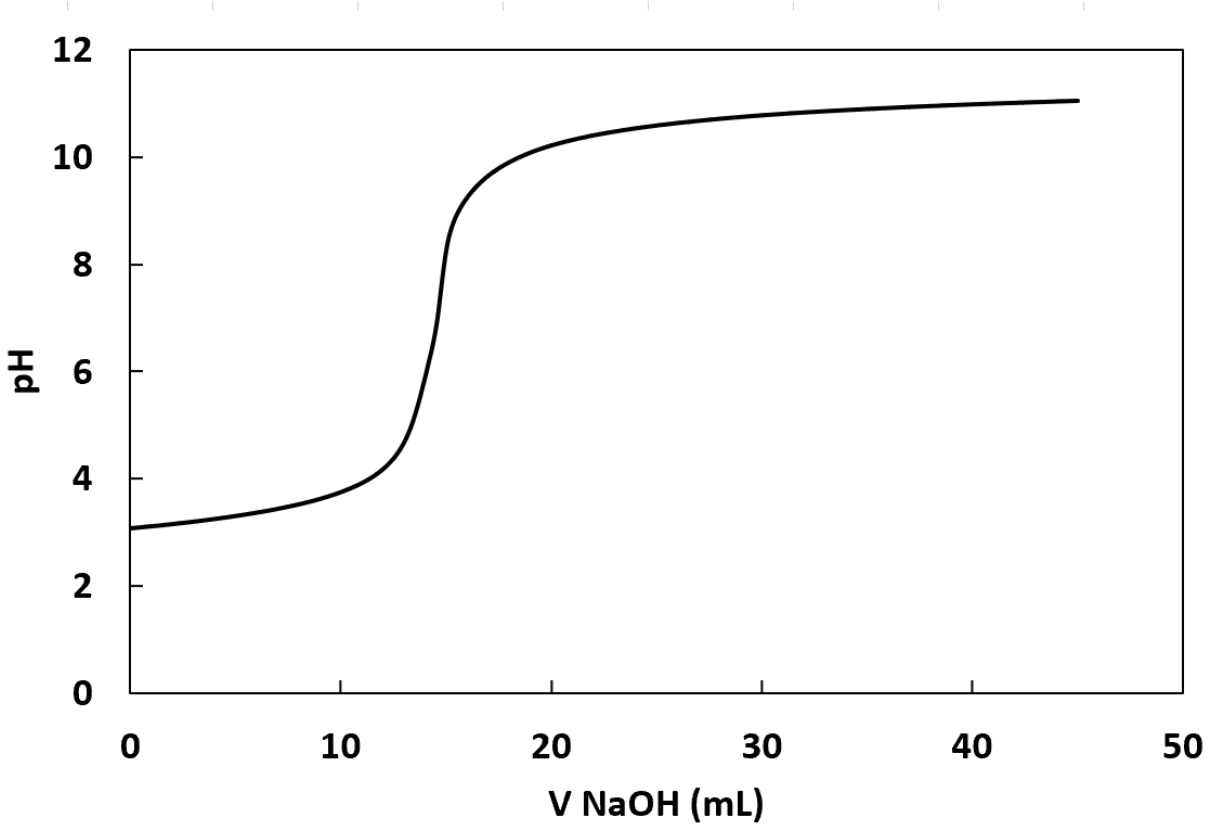

Figure 9: Conductometric Titration pH Curve of Sample Filter Paper Microfibers

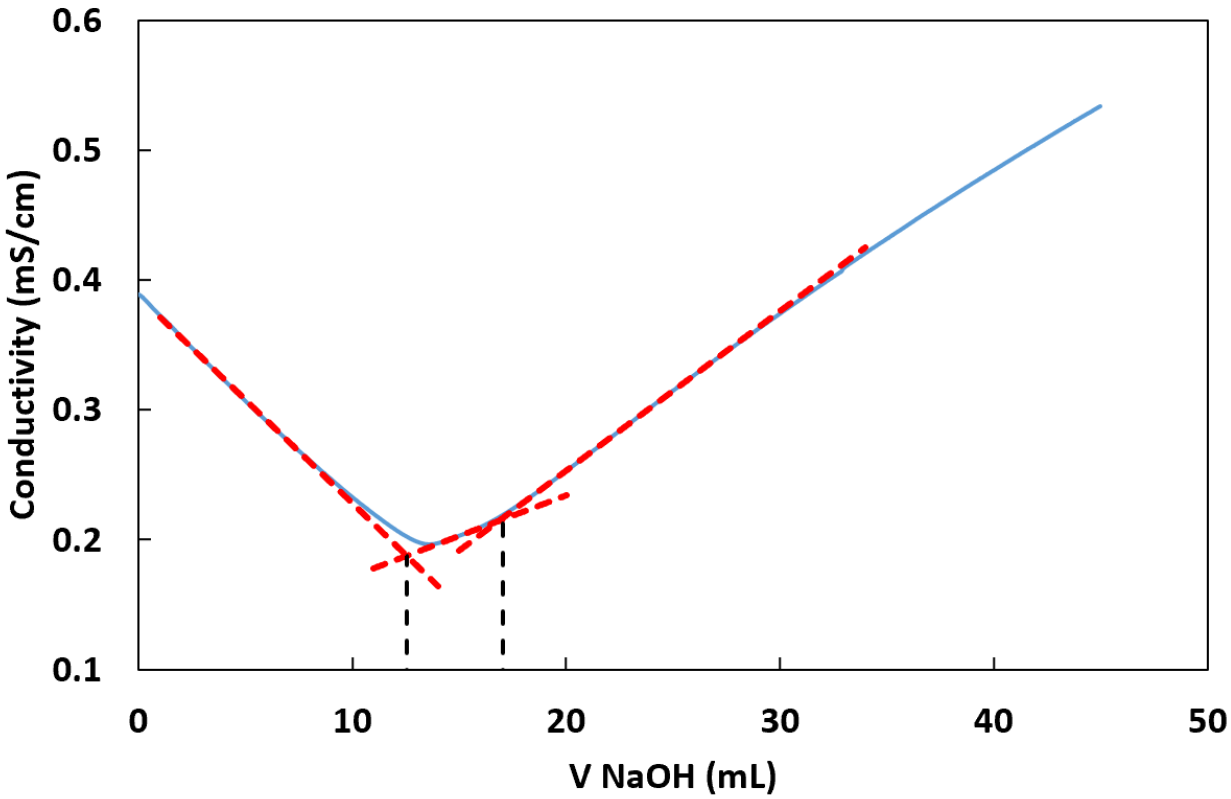

Figure 10: Sample Conductometric Titration of Filter Paper Microfibrous Precipitate

The volume of 10 mM NaOH added in the weak acid region, found by linearizing between each linear conductivity region and finding the volume of NaOH in between these two region's intersections at the tangent to both curves allows the carboxylate content to be calculated as seen in **Figure 11**.

V NaOH consumed	4.53	mL
NaOH concentration	9.976	mM
Initial Microfibers	0.02	g
Microfibers concentratior	0.633%	w/v
	0.00633	g/ml
Microfibers added	3.160	ml
Water added	136.840	ml
Total volume	140.000	ml
COOH concentration	2.26	mmol/g

Figure 11: Calculation of Carboxylate Content

This procedure for carboxylate content calculation determined the filter paper carboxylated microfibrous precipitate to have 2.26 mmol/g, and this process was repeated to show that the Soft Wood Kraft Pulp microfibrous precipitate had a much higher content, as reflected by a wider weak acid region, of 4.22 mmol/g.

The aldehyde content of the respective DAMC fibers oxidized to make these carboxylated microfibrous precipitate products were also determined through a similar conductometric method that instead uses a hydroxylamine hydrochloride titration.[71] Using this method, the filter paper DAMC was shown to have an aldehyde content of 5.28 mmol/g while the Soft Wood Kraft pulp DAMC had 7.62 mmol aldehyde/g.

III. Light Microscopy of Carboxylated Cellulose Microfibrous Precipitate

In order to further characterize the carboxylated cellulose microfibrous precipitate of both the Whatman Filter Paper and the Soft Wood Kraft Pulp cellulose, light microscopy images were taken to show the physical shape of the fibers and show that they were phase separated. Phase separation is a critical property for adsorbents because it achieves more ease of separation from the water medium in

order to separate bound antibiotic from solution more efficiently. Considering the microfibrous precipitate is just that, a microfibrous precipitate of cellulose that separated without ethanol addition, it was expected that the fibers would be long and viewable under light microscopy, as confirmed in **Figure 12**.

a.

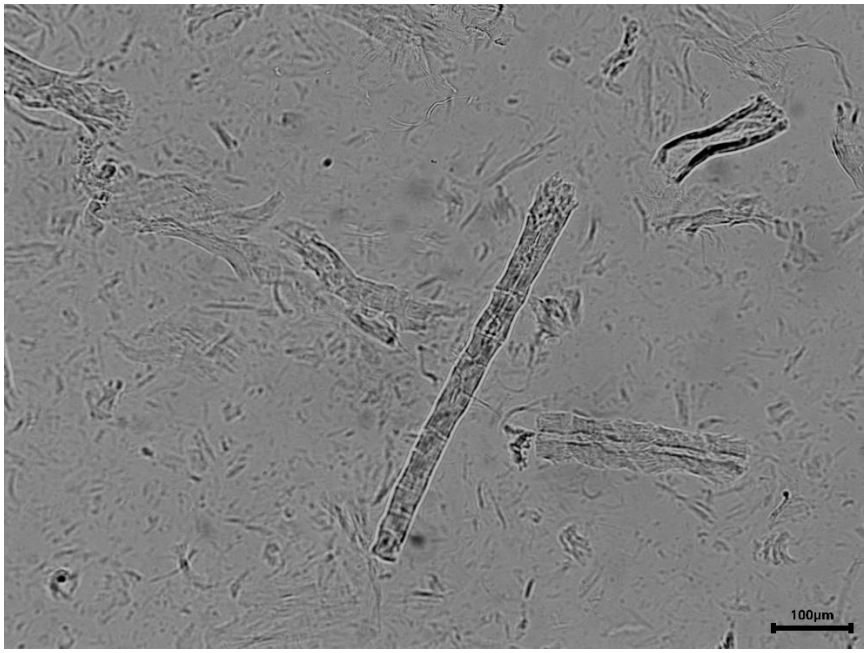

b.

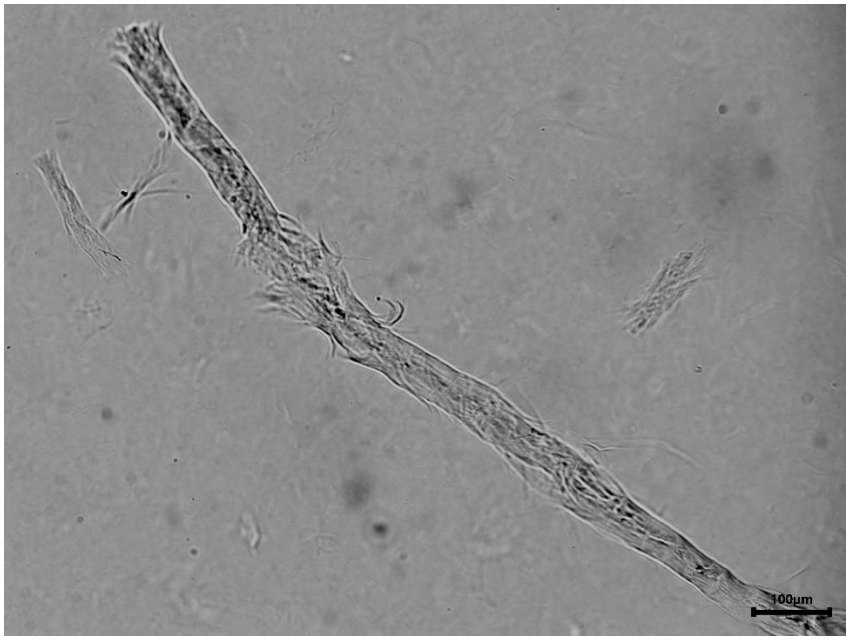

Figure 12: Light Microscope Images of Carboxylated Cellulose Microfibrous Precipitate of (a) Whatman Filter Paper and (b) Soft Wood Kraft Pulp

IV. Vancomycin Calibration Curve

To assess the concentration of vancomycin remaining in each sample using the absorbance and Beer-Lambert's Law, first the wavelength of maximum absorbance was determined by an absorbance scan from 200 nm to 800 nm for numerous concentrations from 0.08 to 10 mg/mL, as seen in **Figure 13**. The second major peak was utilized, at 280 nm, rather than the original peak near 200 nm since the initial peak would overshoot the absorbance limit, and so 280 nm was set as the wavelength for all absorbance studies, creation of calibration curves for vancomycin, and concentration determination after removal studies.

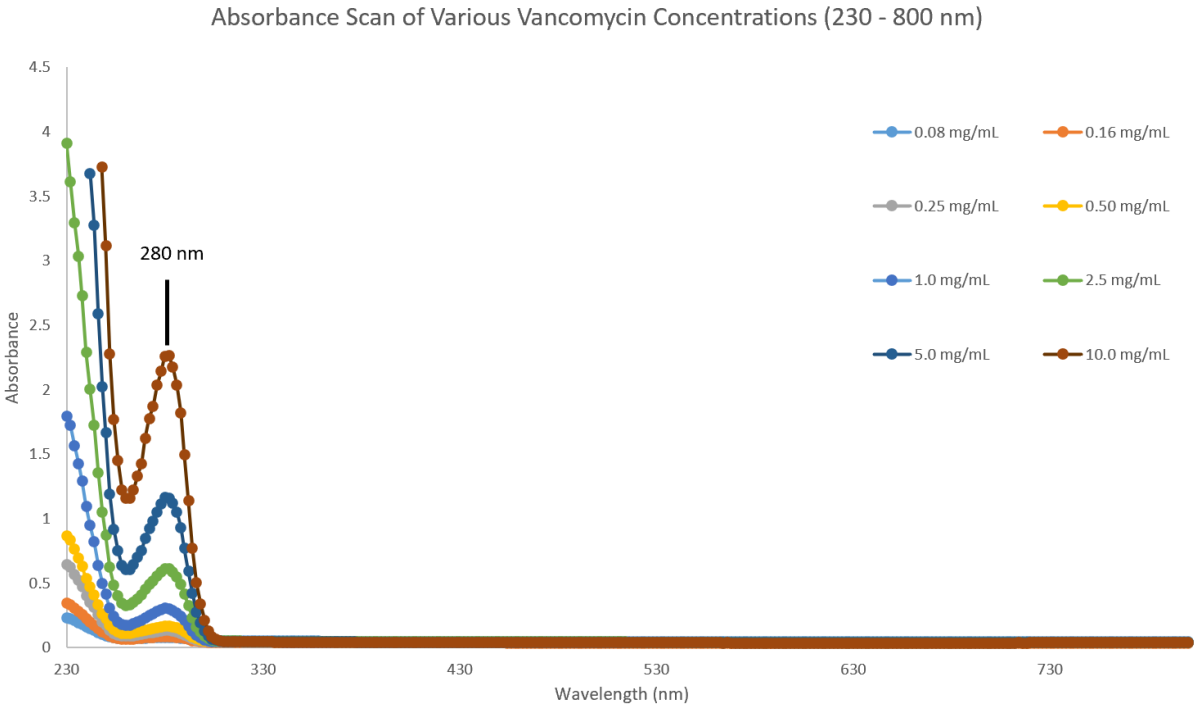

Figure 13: Absorbance Scan of Vancomycin (200 - 800 nm)

Using 280 nm as the peak wavelength, various concentrations of vancomycin were linearized to create a calibration curve such that the absorbance could be used to directly correlate to determine concentration using Beer-Lambert's Law (**Equation 1)**

$$A = \varepsilon * b * c$$ **Equation 1**

where A represents the absorbance, ε is the molar absorptivity or molar attenuation coefficient, b represents the path length between the detector and the sample, and c represents the concentration. Since the path length and molar absorptivity are fixed, the relationship between absorbance and concentration are linear and can be plotted as such, which was done in the calibration curves obtained for vancomycin in **Figures 14, 15,** and **16** for high, medium, and low concentrations of vancomycin respectively. The calibration curves each accounted for slight non-zero absorbance of samples without antibiotic present, tracing back to a non-zero intercept, using the plate reader for all absorption trials.

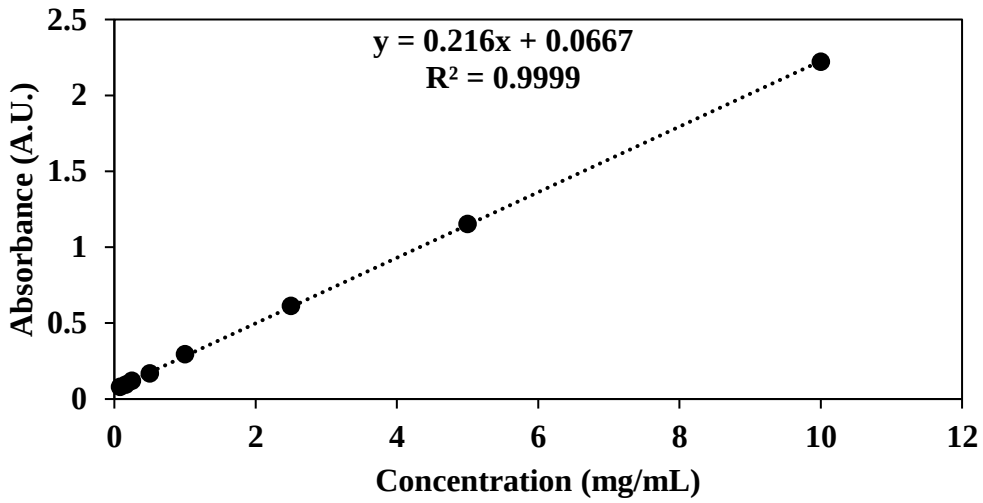

Figure 14: High Concentration Calibration Curve of Vancomycin

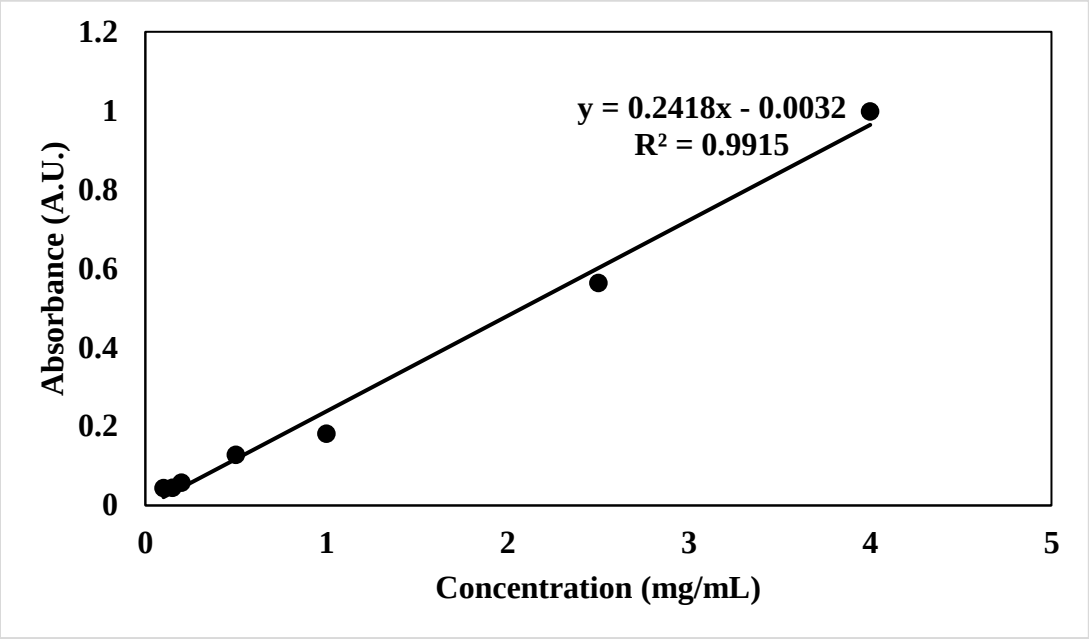

Figure 15: Medium Concentration Calibration Curve for Vancomycin

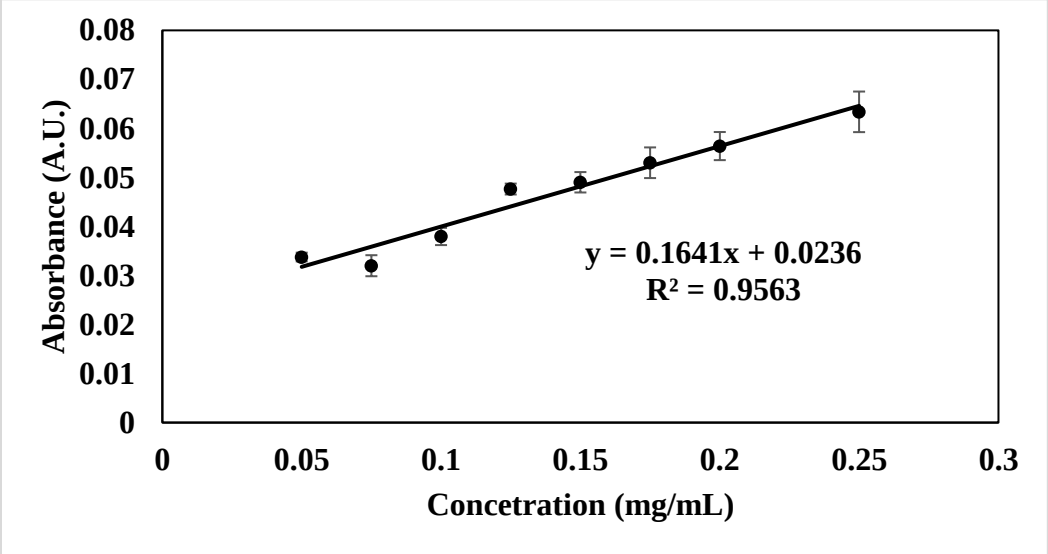

Figure 16: High Concentration Calibration Curve for Vancomycin

The high and medium concentration curves were shown to be very linear, as evidenced by their R^2 values near 1, and as an accurate representation of concentration, but the low concentration curve was less accurate, leaving a detection limit of approximately 1 mg/mL.

V. Linezolid Calibration Curve

Similar to the process of creating calibration curves for vancomycin, first, the maximum wavelength of linezolid was determined by scanning various concentrations from 230 to 800 nm to yield a maximum at 252 nm as shown in **Figure 17**.

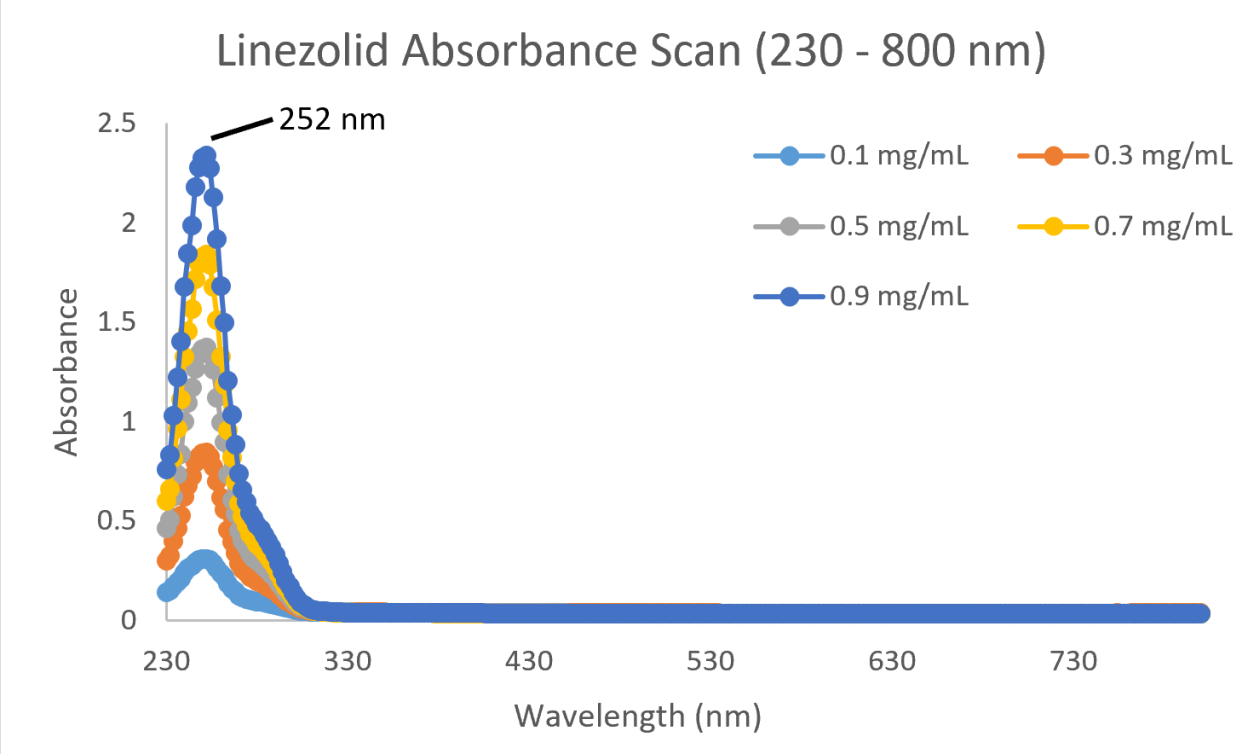

Figure 17: Absorbance Scan of Various Concentrations of Linezolid (230 - 800 nm)

Knowing the maximum absorbance of linezolid at 252 nm, the concentration-absorbance dependence was then determined by plotting the calibration curve in various concentration ranges. Since linezolid has a far stronger fluorophore than vancomycin, lower concentrations were more accessible with the highest concentrations being 2 mg/mL before overshooting the absorbance maximum. **Figures 18, 19**, and **20** show the calibration curves for linezolid at high, medium, and low concentrations, showing accuracy between 0.015 and 1.5 mg/mL.

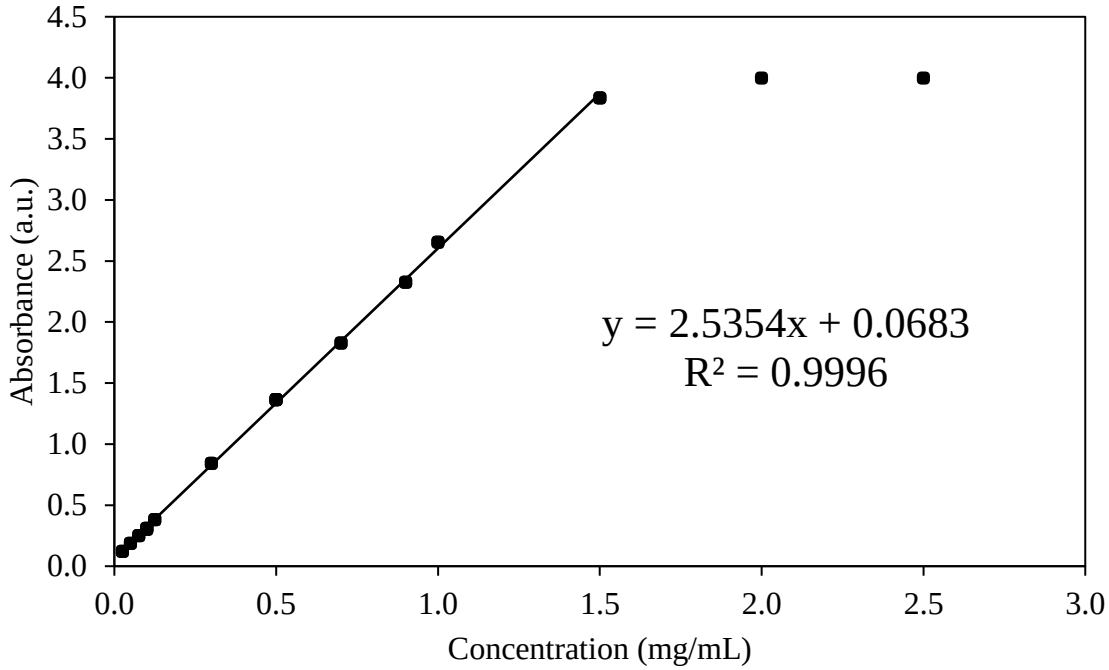

Figure 18: High Concentration Calibration Curve of Linezolid

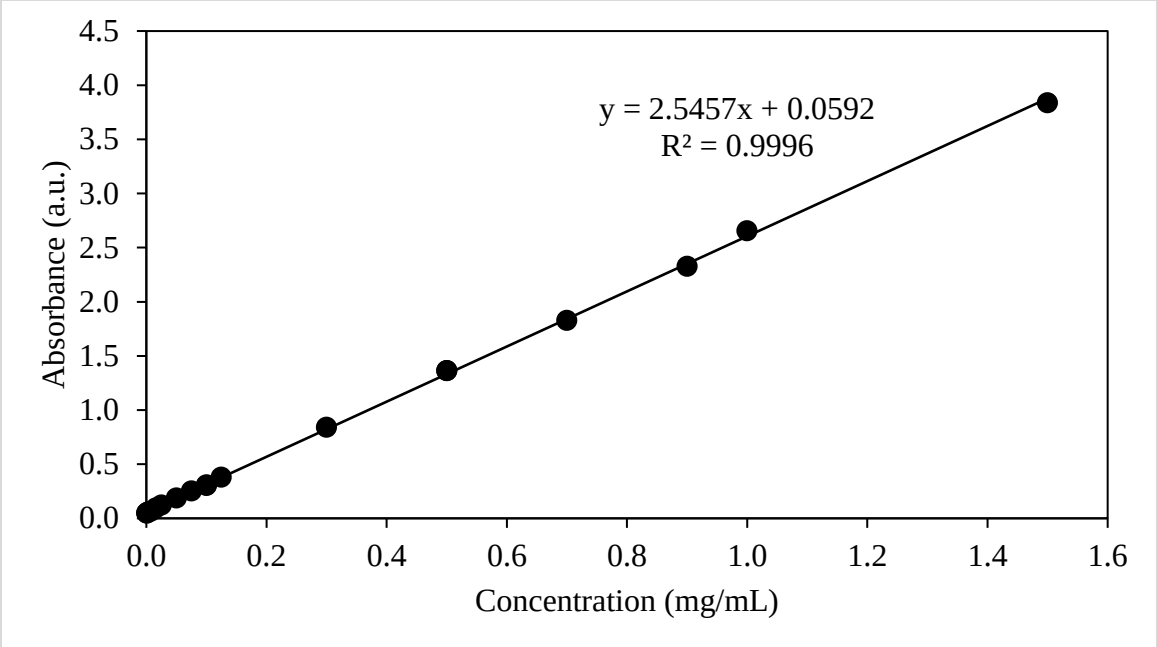

Figure 19: Medium Concentration Curve of Linezolid

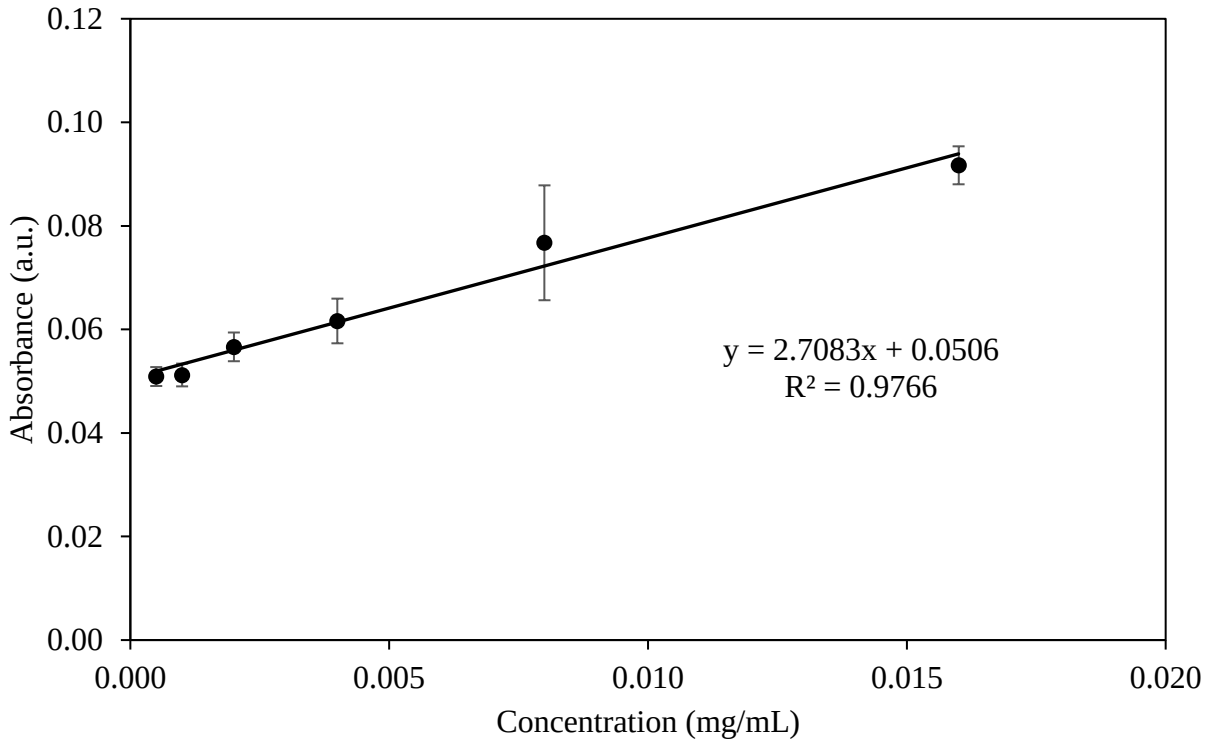

Figure 20: Low Concentration Calibration Curve of Linezolid

VI. Removal Studies

To study the removal ability of functionalized nanocellulose microfibrous precipitates for both vancomycin and linezolid, a protocol for removal studies was developed. First, a concentrated stock of the antibiotic was prepared; this concentration was 25 mg/mL for vancomycin due to its lower absorbance strength and higher water solubility, while linezolid was prepared as a stock of 2.5 mg/mL due to its stronger absorption at lower concentrations and solubility limit at 3 mg/mL.[72] Then, after deciding on the desired concentrations or both adsorbent and antibiotic, into a 1 mL centrifuge tube was added the desired volume of antibiotic stock solution to dilute to the final concentration. The calculated distilled water volume to leave enough for the desired cellulose addition to yield exactly 1 mL was then added and then vortexed

to enable homogeneity. Finally, the cellulose microfibrous precipitate was added to the solution in the calculated amount to the desired volume of 1 mL. Each concentration value was performed in triplicate to ensure result consistency and enable error bar calculation. Each centrifuge tube was then vortexed for 2 minutes on medium to properly mix the solutions, and then the centrifuge tubes were each sealed and centrifuged for 10 minutes at 13,000 rpm. Precipitate formation at the bottom of the centrifuge tube indicated binding and coming out of solution, and so when measuring the concentration of the solution, it was ensured that the top was measured. Finally, using a Tecan i-Control Infinite 200 Pro plate reader at the previously determined maximum absorbance wavelength, 2 μL of each solution was pipetted into a well plate reader and the absorbance values for each solution were recorded. The previously determined calibration curves for each concentration region were then used to determine the concentration of vancomycin or linezolid present in the solution after removal using the adsorbent.

VII. Removal Capacity and Removal Percentage Calculations

Removal capacity and removal percentage are the main metrics used to compare adsorbents, with removal capacity being most universal due to it not depending on mass of adsorbent added and merely being the amount of contaminant removed per gram of material. Now that the concentrations of the antibiotics in each solution are known, both removal capacity and removal percentage can be calculated readily. Removal capacity is calculated using **Equation 2,**

$$\textbf{Removal Capacity}\left(\frac{\textbf{mg antibiotic}}{\textbf{g adsorbent}}\right) = \frac{(C_o - C_e)V}{m} \qquad \textbf{Equation 2}$$

where C_o is the initial concentration of the antibiotic, C_e is the equilibrium concentration of the antibiotic after removal as determined by absorbance, with both concentrations being in mg/mL, V is the volume of the solution (in this case, fixed at 1 mL), and m represents the mass of carboxylated microfibrous precipitate added.

Similarly, removal percentage was calculated for each removal experiment using **Equation 3,**

$$\textbf{Removal Percentage} = \frac{C_o - C_e}{C_o} * 100\% \qquad \textbf{Equation 3}$$

where C_o and C_e represent the initial and equilibrium concentrations of antibiotic.

The removal capacities at different concentrations could then be graphed versus the equilibrium concentration to yield a Langmuir monolayer adsorption isotherm, while the removal percentages were plotted against initial concentration in the figures created for this work, following literature convention.

4. Results and Discussion

I. Vancomycin

Vancomycin is a critical antibiotic of last-resort, which also happens to be cationic, a property which makes it an apt target for anionic cellulose derivatives, and as a result, much of the antibiotic removal in this work will target vancomycin.

I. Selection of a Cellulose Source: Whatman Filter Paper of Softwood Kraft Pulp

To first determine the higher performance nanocellulose microfibrous precipitate cellulose source, Whatman filter paper derived microfibers and those made from Softwood Kraft pulp were tested with a fixed 1 mg/mL of vancomycin at various masses of microfibrous precipitate adsorbent. The baseline was set as a one-to-one stoichiometric concentration between negatively charged carboxylates of the microfibers and positively charged amines of vancomycin, since electrostatic interaction is the predicted mode of binding. Since the Softwood Kraft pulp microfibrous precipitate has nearly twice as much charge content (4.22 mmol/g) as the microfibrous precipitate of filter paper (2.26 mmol/g), the filter paper microfibers mass was set as the baseline, as 0.3 mg fibers for a 1:1 stoichiometric interaction according to **Equation 4:**

$$\boldsymbol{Charge\ content\ vancomycin} = \frac{\mathbf{1}\ \boldsymbol{mmol\ amine}}{\boldsymbol{MW_{vancomycin}}} * \boldsymbol{m_v} = \boldsymbol{Charge\ content\ fibers}$$

$$= \mathbf{carboxylate\ content}\left(\frac{\mathbf{mmol}}{\mathbf{g}}\right) * \mathbf{m_f(g)} \qquad \textbf{Equation 4}$$

where m_v is the mass of vancomycin while m_f is the mass of fibers (each standardized to 1 mL of volume) so the mass is the same as the concentration in mg. Thus, the initial trials of were determined for microfibrous precipitate of filter paper and Softwood Kraft pulp to get a baseline of which adsorbent is more successful at removing vancomycin; the ratio's began at 1:1 for the less carboxylated filter paper microfibers and went to a significant excess to see if complete removal of the antibiotic could be achieved, as seen in **Table 3.**

Table 3: Masses of Vancomycin and Microfibrous Precipitate of Each Source to Establish a Baseline and Stoichiometric Charge Ratios.

Vancomycin Concentration (mg/mL)	Mass Microfibrous Precipitate and Cellulose Source	Stoichiometric Charge Ratio Cellulose carboxylate: vancomycin amine
1.0	0.3 mg Filter Paper	1 : 1
1.0	0.3 mg Softwood Kraft Pulp	1.8 : 1
1.0	0.6 mg Filter Paper	2 : 1
1.0	0.6 mg Softwood Kraft Pulp	3.6 : 1
1.0	6.0 mg Filter Paper	20 : 1
1.0	4.3 mg Softwood Kraft Pulp	25 : 1

Despite the expectation being that the Softwood Kraft pulp microfibers would be a superior adsorbent, due to it having nearly double the charge content of the filter paper microfibers, it was found very conclusively that the Softwood Kraft pulp microfibers were far worse at removing vancomycin, as seen by their removal percentages at each mass of adsorbent compared in **Figure 21**.

a.

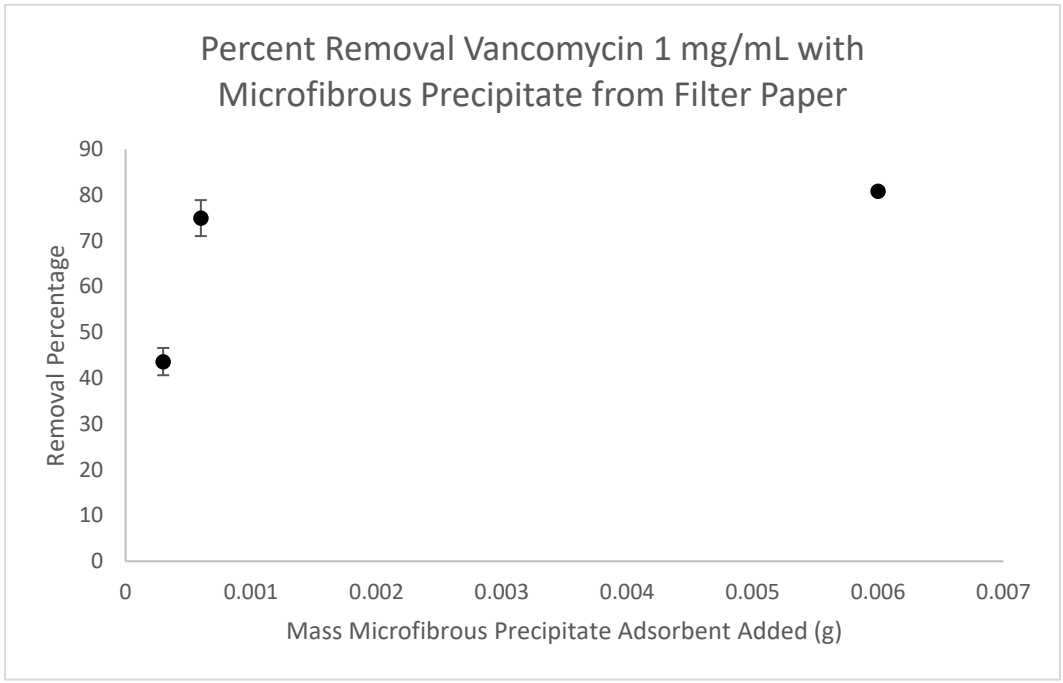

b.

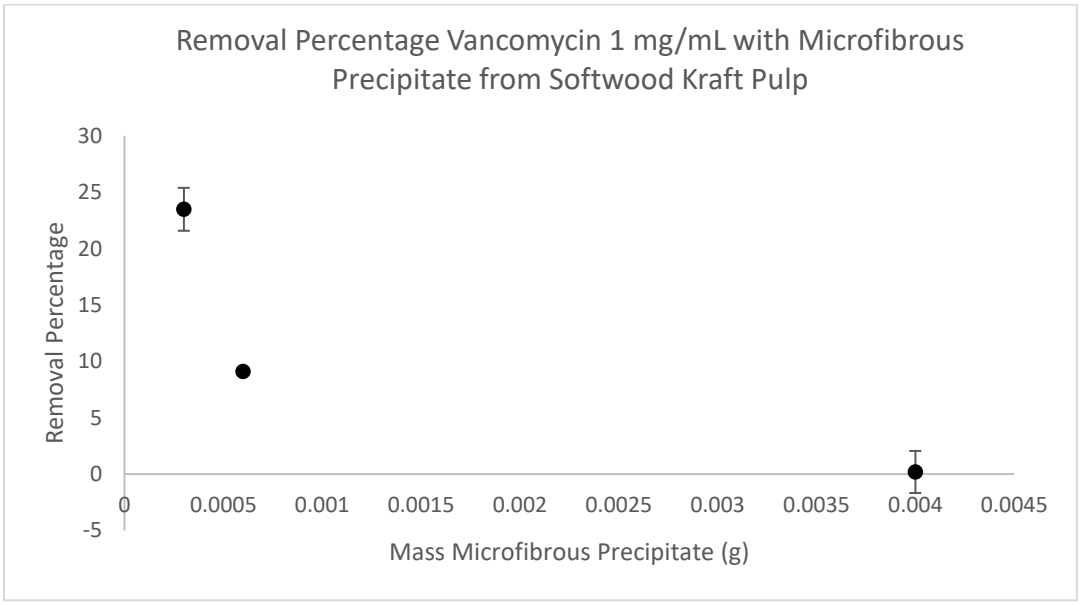

Figure 21: Removal Percentages of Vancomycin from a 1 mg/mL Solution Using Various Masses of Microfibrous Precipitate from (a) Whatman Filter Paper and (b) Softwood Kraft Pulp

These graphs show that essentially no removal occurred of the vancomycin using Softwood Kraft pulp derived microfibrous precipitate, while the filter paper microfibers were much more successful, achieving upwards of 90% removal in excess and still being able to

achieve moderate removals of low concentration (1 mg/mL) of vancomycin at 1:1 stoichiometric ratio. It is predicted that this phenomenon whereby the more carboxylated product removed less is not so much due to a lack of binding affinity since it is clearly expected that the carboxylate will interact with the positively charge amines. Instead, the hypothesis is that due to the fact that filter paper is nearly pure cellulose while Softwood pulp has significant portions of cellulose, the filter paper more cleanly converted to fibers of larger size which were able to phase separate better. **Figure 22** clearly shows how the first, third, and fifth centrifuge tube (each of which had filter paper fibers, increasing in concentration from left to right), precipitated significantly, while the equivalent amounts of the Softwood Kraft pulp microfibers did not precipitate, so larger size and the lower carboxylate content which helps keep the filter paper fibers out of solution may be contributing to the advantages in separation and removal for filter paper.

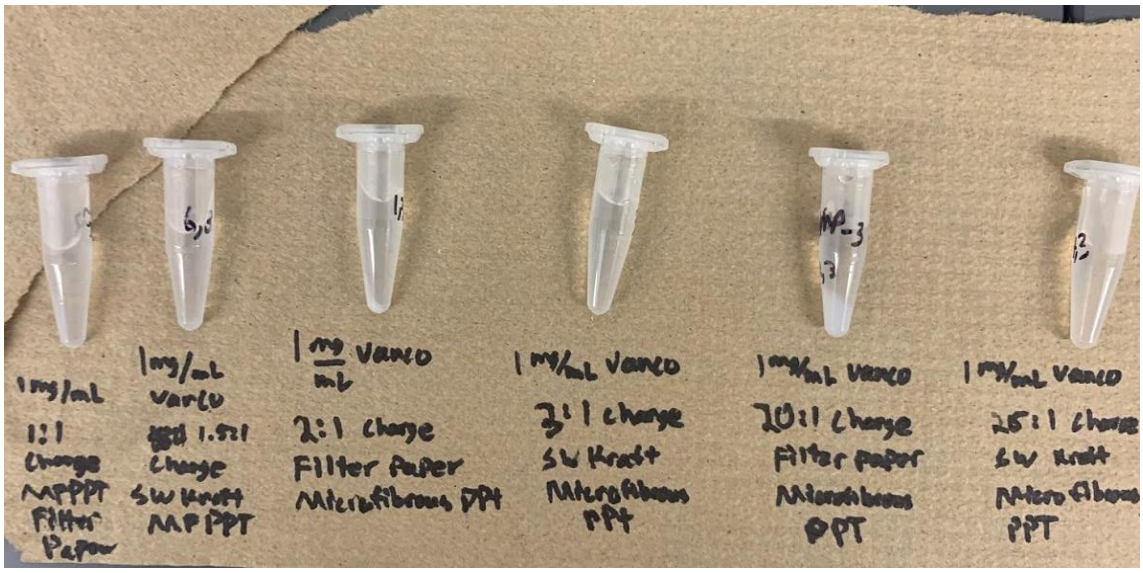

Figure 22: Picture of Filter Paper (1, 3, 5) and Softwood Kraft Pulp (2, 4, 6) Microfibers Removal Experiments for Vancomycin, Increasing in Adsorbent Concentration from Left to Right.

The removal capacities for vancomycin also followed this trend where filter paper was much more successful at removing vancomycin from solution than the microfibers of Softwood pulp, as seen in **Figure 23.**

a.

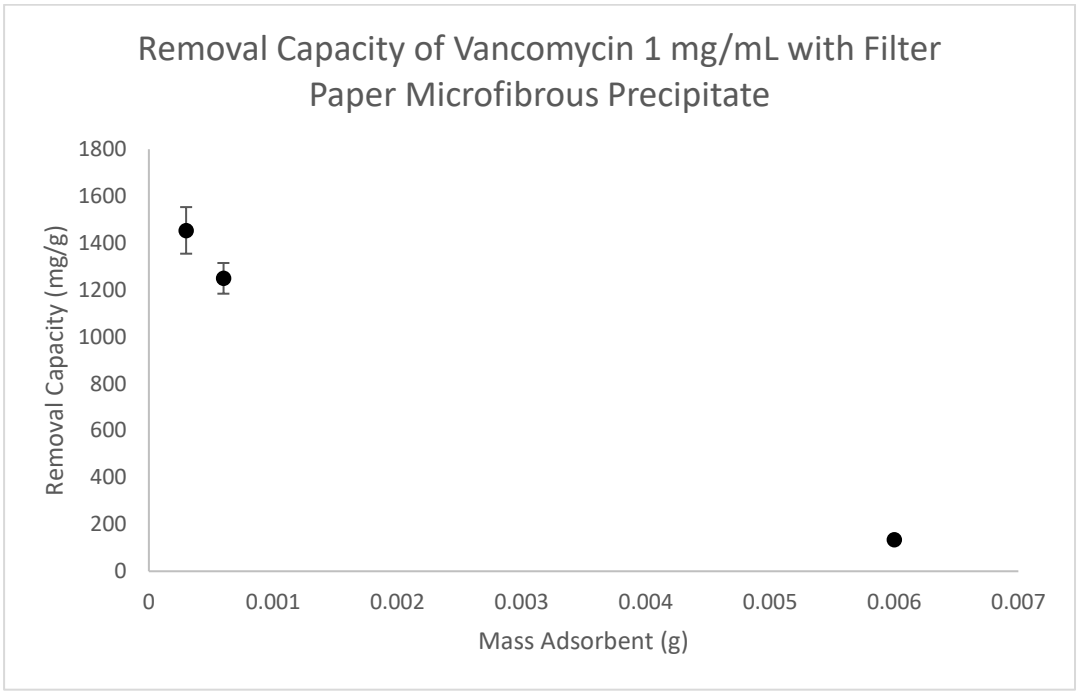

b.

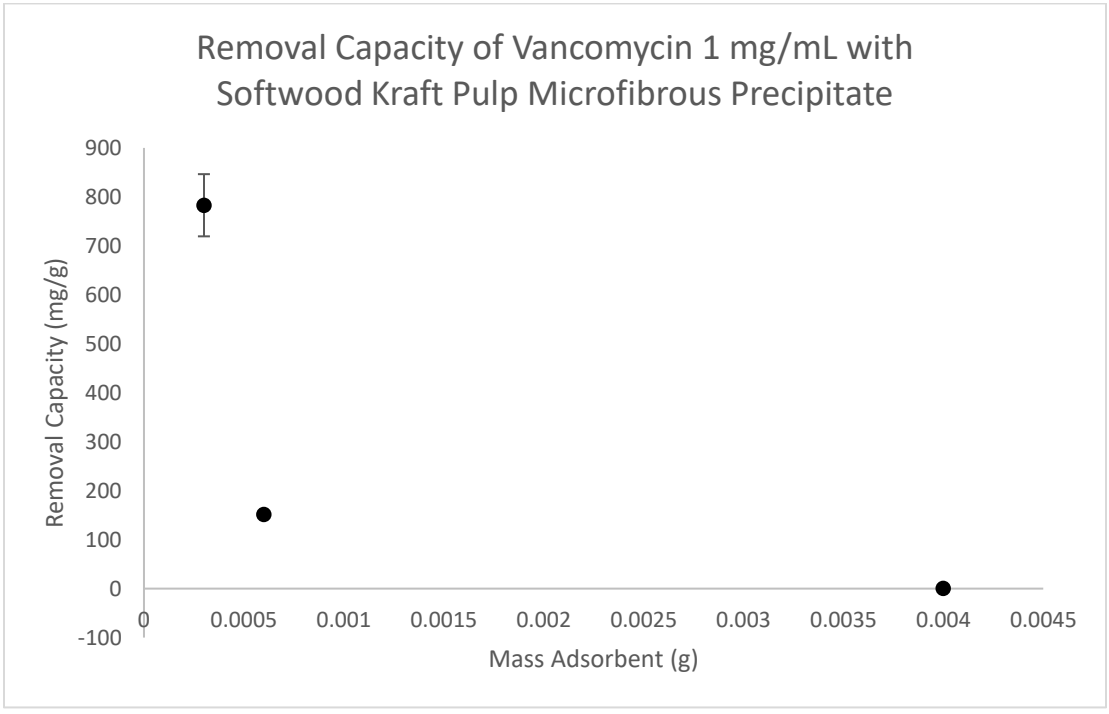

Figure 23: Removal Capacities of Vancomycin from a 1 mg/mL Solution with Carboxylated Microfibrous Precipitate Derived from (a) Filter Paper and (b) Softwood Kraft Pulp

II. Vancomycin Removal with Whatman Filter Paper Microfibers

Now that the filter paper microfibers had experimentally been determined to be superior at adsorbing vancomycin, further experimentation was conducted to test the material and determine the maximum removal capacity as physiological pH, since the eventual goal is to apply a material like this to remove off-target antibiotics from the blood stream to prevent antibiotic resistance from developing. While fixing the mass of the filter paper microfibers this time at 1 mg, the concentration of vancomycin was varied from 0.3 mg/mL to 9 mg/mL while monitoring percentage of removal and removal capacity. **Figures 24** and **25** illustrate these metrics.

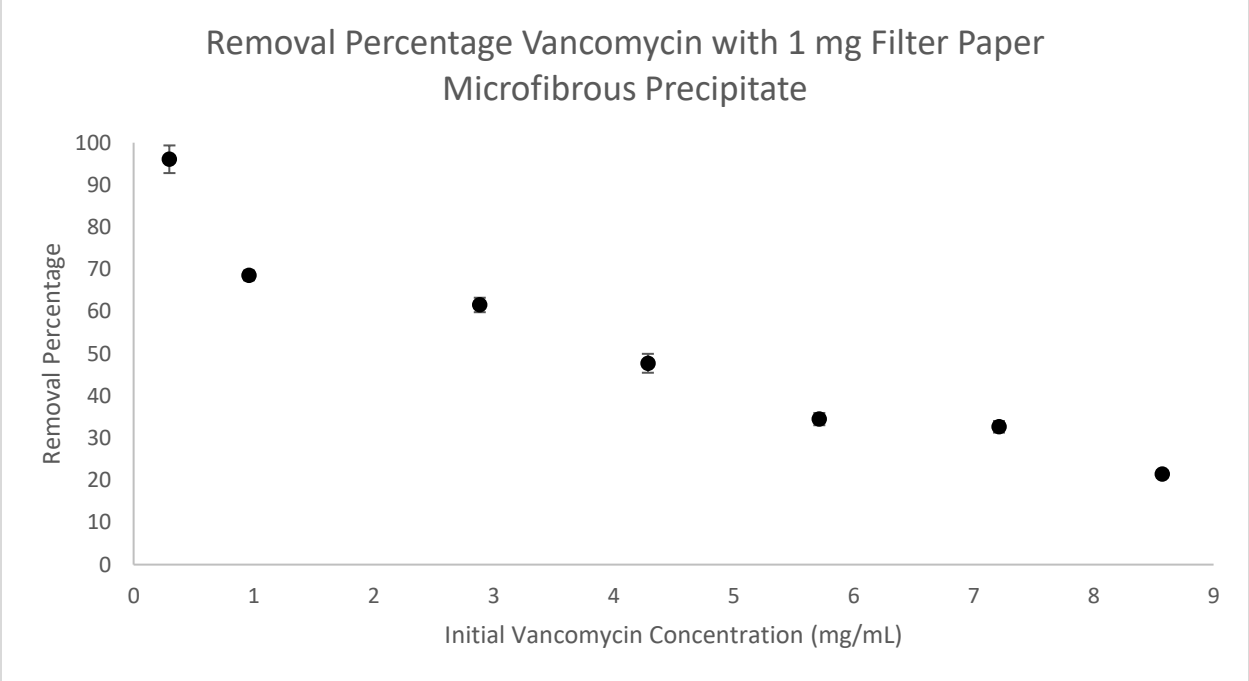

Figure 24: Removal Percentage of Vancomycin with 1mg Filter Paper Carboxylated Microfibrous Precipitate at pH 6.5

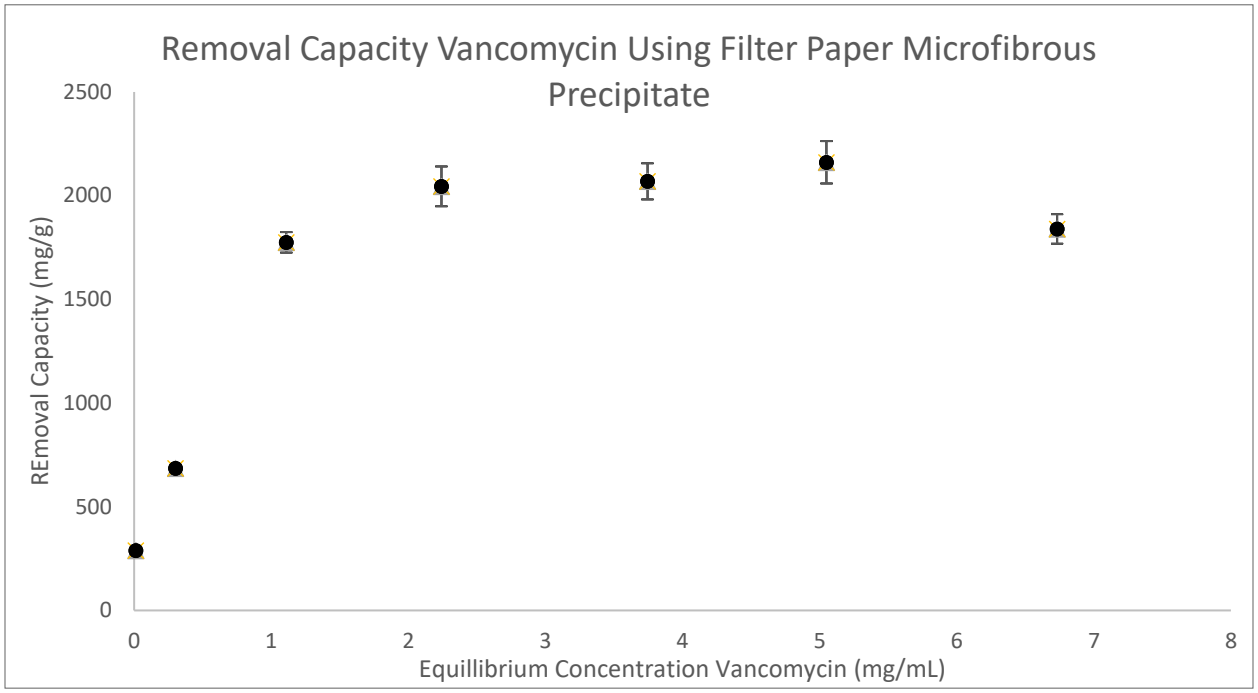

Figure 25: Removal Capacity of Vancomycin by 1 mg of Filter Paper Microfibrous Precipitate at pH 6.5

Both plots of the removal capacity and removal percentage follow the exact expected behavior. The removal percentage drops as expected as more vancomycin is introduced into the solution, overwhelming the adsorbent as seen in **Figure 24**, while at very low concentrations of vancomycin, nearly all of the antibiotic is swiftly removed. When the filter paper carboxylates were in excess (6:1 stoichiometrically) at an initial vancomycin concentration of 0.3 mg/mL, 95% of the antibiotics were removed from solution, which is a notable data point considering this lower concentration removal at a concentration that ENCC would have struggled to achieve.

Figure 26 visually confirms the expected levels of removal by showing the relative precipitation amounts for selected points on the graph. The lower concentration trials, of 0.3 mg/mL and 1 mg/mL vancomycin showed lower removal capacities, and as such, the amount of precipitate seen is not notable. However, above 3 mg/mL, the maximum removal capacity begins to be achieved of nearly 2100 mg/g, and so it is seen in **Figure 26** that the trials for 3 mg/mL, 6

mg/mL, and 9 mg/mL have approximately the same visual levels of removal and as a result, precipitation. Thus, the trend seen in **Figure 26** aligns directly with the quantitative data collected. Above 3 or 6 mg/mL, the removal capacity is accomplished, and so removing more vancomycin from solution is not feasible with the fixed 1 mg of carboxylated filter paper fibers, and so the trend confirms low removal at low concentrations and then the plateau seen in removal capacity.

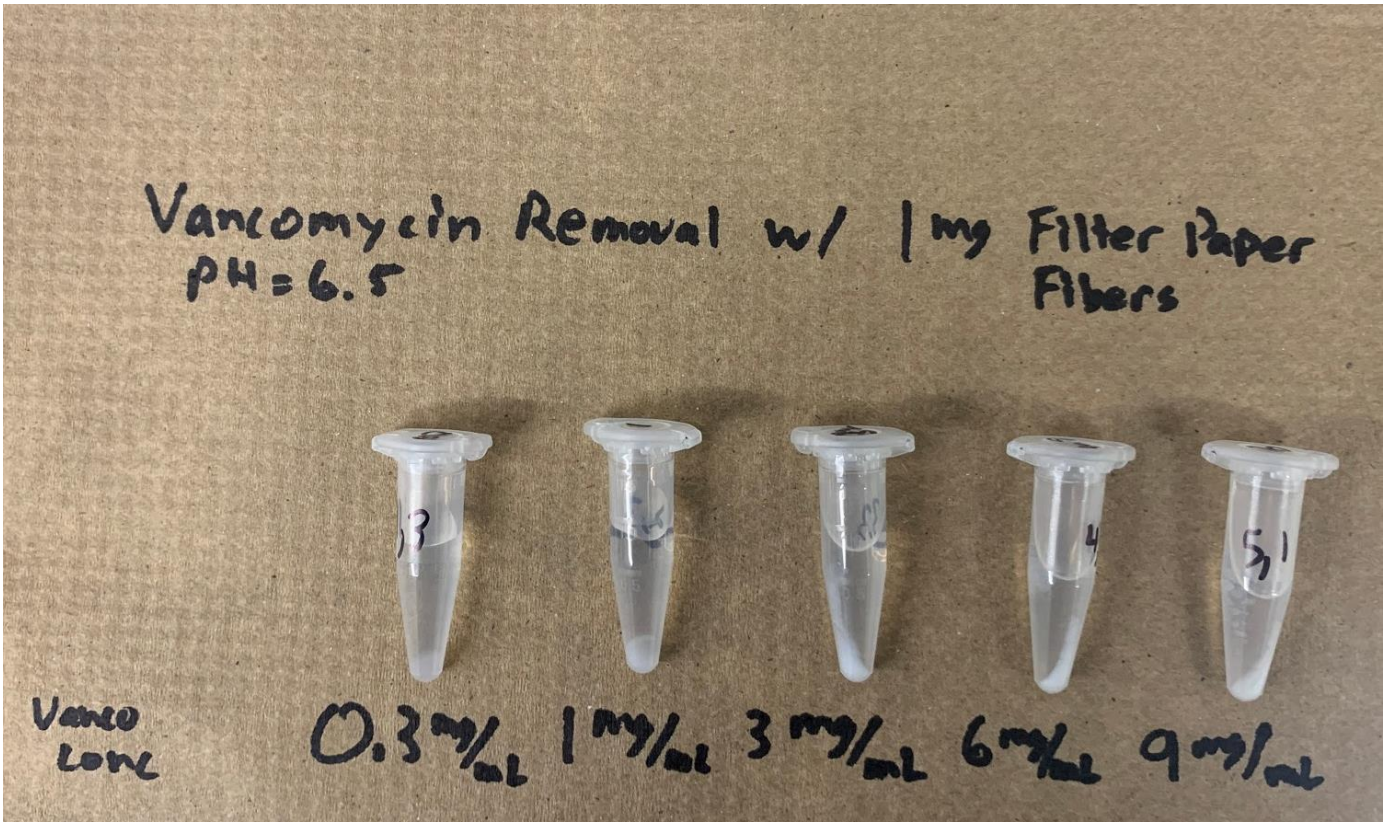

Figure 26: Visual Representation of Precipitation Levels of Vancomycin at Various Concentrations (0.3, 1, 3, 6, 9 mg/mL) Using 1 mg of Filter Paper Fibers

It is no surprise that as the carboxylates of the filter paper fibers were fixed with increasing concentration of vancomycin, the removal percentage dropped since the adsorbent became overwhelmed and outnumbered stoichiometrically, but it still showed the ability to remove some antibiotic for all trials. Removal capacity is seen increasing in a logarithmic shaped

curve, exhibiting saturation behavior, as predicted by adsorption models, before reaching its maximum removal capacity in the range of 2100 mg/g at an equilibrium concentration of vancomycin of approximately 2.5 mg/mL and plateauing. This trend is consistent with the Langmuir monolayer assumptions, and has been linearized to show that the saturation behavior follows the Langmuir isotherm model fairly well in **Figure 27.** The assumptions of the Langmuir model are that adsorption occurs in a single layer, with each site being kinetically and thermodynamically equivalent, meaning there are no adsorbate-adsorbate interactions that may diminish or increase adsorption as coverage increases.[73] This model can be described by the equation,

$$\frac{\mathbf{1}}{\Gamma_{\boldsymbol{e}}} = \frac{\boldsymbol{K}}{\boldsymbol{C_e}} + \frac{\mathbf{1}}{\Gamma_{\boldsymbol{m}}} \qquad \textbf{Equation 5}$$

where Γ_e represents the equilibrium removal capacity experimentally determined, C_e is the equilibrium concentration of vancomycin, K is the equilibrium constant for adsorption, and Γ_m is the maximum removal capacity of vancomycin. From this equation, **Equation 5**, it becomes apparent that linearizing by plotting $1/\Gamma_e$ versus $1/C_e$ yields a line with slope K and intercept $1/\Gamma_m$, as shown in **Figure 27.**

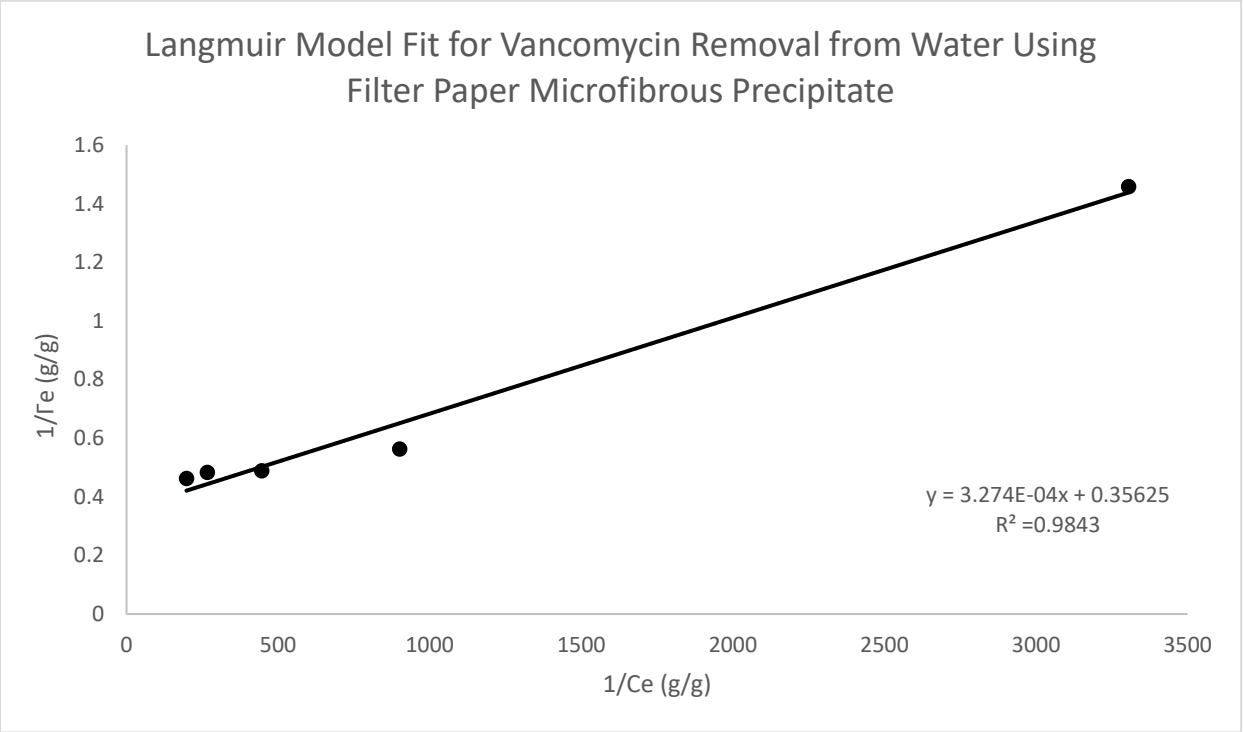

Figure 27: Langmuir isotherm fit for parameter determination for vancomycin removal using filter paper microfibrous precipitate

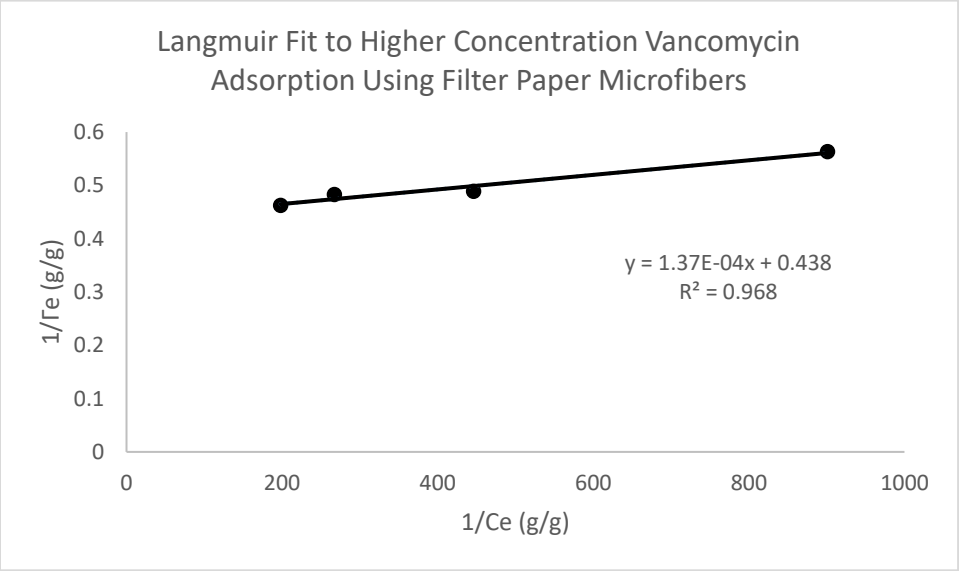

Figure 28: Langmuir isotherm fit for parameter determination at higher concentrations

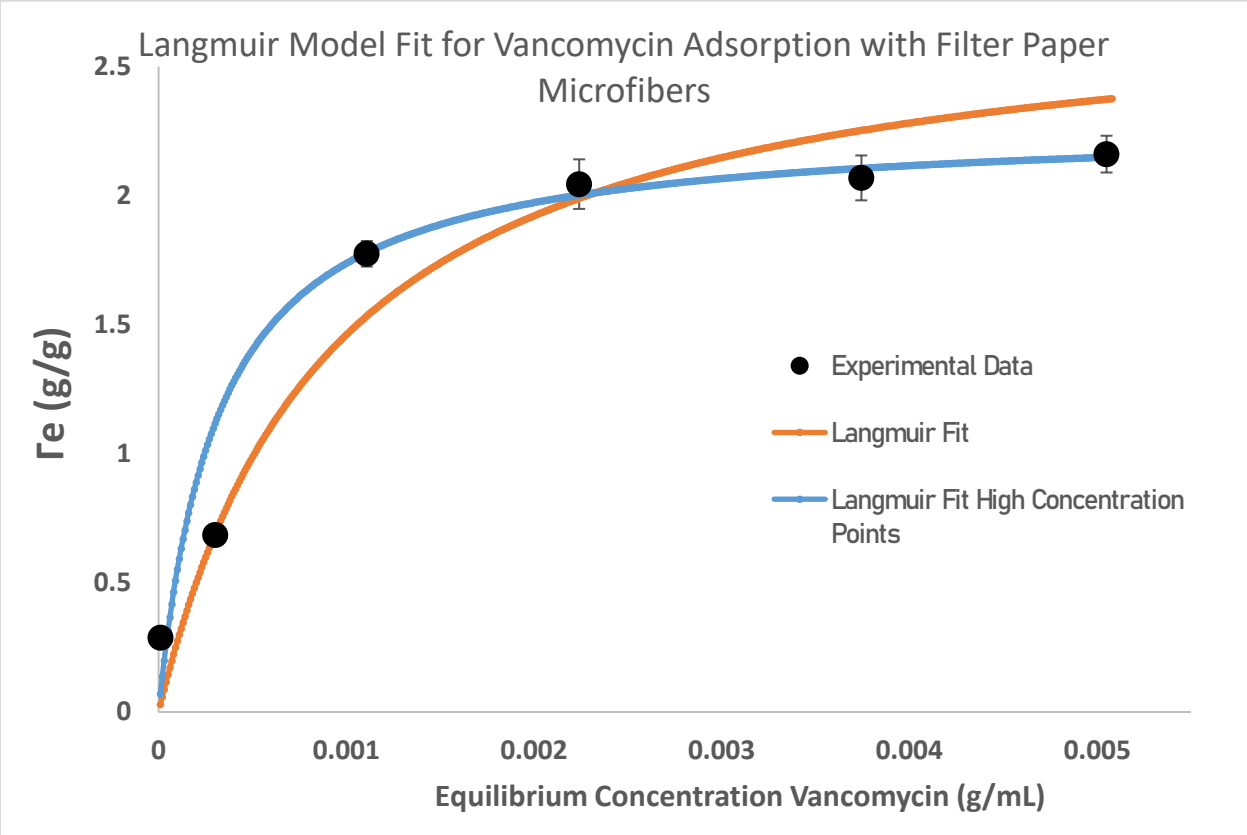

Figure 29: Langmuir model fit for vancomycin adsorption with filter paper microfibers compared to experimental data

The Langmuir equation, presented as **Equation 5**, can be rearranged in terms of equilibrium removal capacity, Γ_e to be plotted against the experimentally acquired data,

$$\Gamma_e = C_e * \left[\frac{1}{\Gamma_m * K} + \frac{C_e}{\Gamma_m} \right] \qquad \textbf{Equation 6}$$

where Γ_e can be plotted compared to the empirically determined Langmuir parameters, K and Γ_m, to analyze the aptness of the Langmuir fit, as seen in **Figures 27** and **28**.

Thus, from the Langmuir fit, for the adsorption of vancomycin from water solution using Whatman filter paper microfibrous precipitate, it can be seen that the equilibrium constant, K, is $3.274 * 10^{-4}$ while Γ_m= 2.81 g vancomycin/g microfibers. The fit, though, appears to have a different linear region in the higher concentration regime (lower $1/C_e$) that does not perfectly align with the lower concentration points, and so the parameters were recalculated by linearizing

while discarding this data point, in **Figure 28**, where Γ_m = 2283 mg vancomycin/g microfibers and K = 1.37 * 10^{-4}. The maximum removal capacity of 2283 mg/g is in much stronger alignment with the experimentally determined maximum removal capacity of approximately 2200 mg/g, and as a result the plot found with these parameters, indicated in blue in **Figure 29**, fits much better. Regardless, the results of both plots are shown in **Figure 29** to illustrate that the Langmuir model overall represents this situation fairly well.

The fitting of the Langmuir model indicates that the assumptions that this model was derived under hold to a significant degree; namely, those assumptions include that a monolayer forms, that each site is identical, and that adsorption is not interrupted by adsorbate-adsorbate interactions.[74] The idea that a monolayer would represent the maximum saturation of positively charged vancomycin on carboxylated microfibrous precipitate of filter paper is expected; since electrostatic interaction is responsible for the adsorption, there is no driving force for more positively charged vancomycin to bind to the now positively charged surface due to vancomycin covering the carboxylate sites. As such, a monolayer would represent the maximum, as expected under the Langmuir model. Each site can also be considered identical, since cellulose is a uniform polymer, and the oxidation reactions to incorporate the carboxylate groups should proceed similarly on any site to produce the same carboxylate environment. However, some of the non-ideality found in deviance of the data from the Langmuir model can be attributed to adsorbate-adsorbate interactions, which are present in repulsive interactions between positively charged vancomycin molecules bound to the cellulose. Despite this potential reason for deviation, the adsorption clearly fits a Langmuir isotherm model, and as a result, supports the expectation that adsorption forms in a monolayer.

The removal capacity graph, **Figure 25**, shows a maximum removal of 2161 mg vancomycin/g adsorbent at pH 6.5, which is far superior to all other reported adsorbents, the highest of which achieved a removal capacity of 861 mg/g using Mono-dispersed mesoporous hollow carbon (MHC) nanospheres, nearly outdoing this material three-fold, as seen in **Table 4**.[75]

Table 4: Literature Values of Removal Capacity of Vancomycin from Water for Various Functionalized Adsorbents

Adsorbent Type	**Removal Capacity (mg/g)**
Glycidylmethacrylate modified cellulose	12.9 mg/g [76]
Glycidylmethacrylate modified cellulose with 1 carbon diamines	27.8 mg/g [76]
Glycidylmethacrylate modified cellulose with 3 carbon diamines	37.8 mg/g [76]
Polymeric Supernatant	97 mg/g [77]
Carboxyl Terminated Nanodiamond	125.81 mg/g[78]
Amine Terminated Nanodiamond	183.95 mg/g[78]
Nanodiamond	288.67 mg/g [78]
Polyethyleneglycol based microparticles (MPs)modified with D-Ala-D-Ala-OH ligand	510 mg/g [79]
Column packed with D,L-alanine-immobilized adsorbent	652 mg/g [80]
Crosslinked poly(N, N-dimethylacrylamide) modified with D-Ala-D-Ala	768 mg/g[81]
Mono-dispersed mesoporous hollow carbon (MHC) nanospheres	861 mg/g [75]
Nanocellulose Carboxylated Microfibrous Precipitate	**2116 mg/g**

III. Elucidation of a Removal Mechanism: DAMC Test and pH Variation

To further elucidate the removal mechanism of vancomycin by the filter paper microfibers, a number of experiments varying the factors at play for electrostatic interaction were performed. Since it is hypothesized that the negatively charged carboxylate groups of the filter paper microfibers bind to the positively charged amines of vancomycin, each of these factors was modified to confirm these expectations. First, the rather than attempting to adsorb vancomycin with the fibrous biproduct of the oxidation of dialdehyde modified cellulose (DAMC), the DAMC itself, with only aldehyde groups and no carboxylate groups was tested as an adsorbent for vancomycin. As a proof-of-concept trial, only one point was selected, with an excess of vancomycin so that the DAMC fibers would have the best opportunity to remove since they would always be surrounded by vancomycin. **Table 5** shows just how unsuccessful the DAMC fibers were at removing vancomycin from water compared to the carboxylated microfibers.

Table 5: Removal Capacities of Filter Paper Microfibers and DAMC Fibers for 7.5 mg/mL of Vancomycin in Water

	Removal Capacity			
Trial	DAMC	Filter Paper Microfibers	Average FP (mg/g)	Stdev
1	66.722	2054.131311	2161	102
2	0.000	2257.8346	Average DAMC (mg/g)	Stdev
3	-29.251	2171.260509	12.5	49.2

In fact, the DAMC fibers amounted to a removal capacity of 12.5 $\pm$ 49.2 mg vancomycin/gram, which is nominally zero removal. Comparatively, the filter paper microfibers achieved a removal capacity of 2161 $\pm$ 102 mg/g, indicating that the functionalization of the DAMC with a chlorite oxidation to implement carboxylate groups is the reason that removal is

being achieved. The removal capacity found in this trial for the filter paper microfibers served as an effective control, confirming the removal capacity reported as 2116 mg/g. As such, the mechanism of action can be confirmed as through electrostatic interaction between the negatively charged adsorbent and positively charged antibiotics at pH 6.5 (as a physiologically relevant pH), but pH is another significant parameter for the altering of charge states in solution.

Due to the effects of the surrounding proton concentration on the protonation states of acidic or basic groups on molecules, as indicated by pH as the negative log of the concentration of H^+, pH is another logical variable to identify the mechanism of action as electrostatic interaction. It would be expected that at low pH values, where the concentration of H^+ is high, that the carboxylic acid groups on the cellulose microfibers would be protonated and thus neutrally charged. Generally, carboxylic acids are known to have pKa values of between approximately 3.5 and 5, varying slightly depending on the electronics and other properties of the functional groups surrounding the carboxylic acid carbon.[82,83] Different types of oxidized cellulose such as oxidized cotton cellulose at 4.0 and cellulose oxidized by TEMPO with a pKa value of 3.6.[84,85,86] Thus, since pKa is also on a logarithmic scale like pH, this indicates that at pH values below approximately 4, 50% of the carboxylates on the cellulose microfibers are protonated, and at pH 2, 99% of them are protonated in the neutral form. Similarly, above pH values of 6, 99% of the carboxylates on the cellulose microfibers are expected to be deprotonated, in the active negatively charged form for adsorption, meaning that little changes to the adsorbent will take place above the pH of 6.

Vancomycin protonation state will also vary with pH because it has one primary amine, one secondary amine, and one carboxylic acid group as seen in its structure in **Figure 30**.

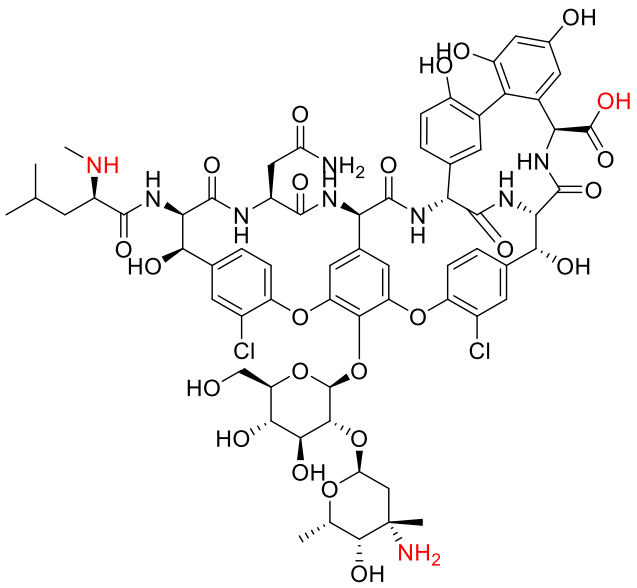

Figure 30: Structure of Vancomycin with Acidic and Basic Groups Indicated

For simplicity, the carboxylic acid and secondary amine can essentially shield each other's charge leaving just a weakly basic primary amine that dictates the charge of the molecule. The conjugate acid of this primary amine, its protonated form, has a pKa of 7.8, meaning below pH values of 7.8, more than 50% of vancomycin molecules are positively charged, with slight additional contribution from the other amine, while above pH of 9.8, vancomycin is neutrally, or in fact, negatively charged due to the deprotonation of the carboxylic acid, making higher pKa values a poor range for removal using a negatively charged cellulose due to repulsion.[87] Thus, it is expected that in the pH range between 5 and 7, vancomycin will be removed best using carbxoylated cellulose microfibers while the removal will drop sharply above pH 9 or below pH 3. This hypothesis was tested by adjusted the pH of trials of vancomycin concentration of 6 mg/mL at pH 1.5, 3, 5, 7, 9, and 12, each within 0.1 pH units. The pH was adjusted before and after addition of the cellulose fibers to ensure that removal occurred at the designated pH, and the removal capacity was plotted in **Figure 31** with associated removal percentages shown in

Figure 32.

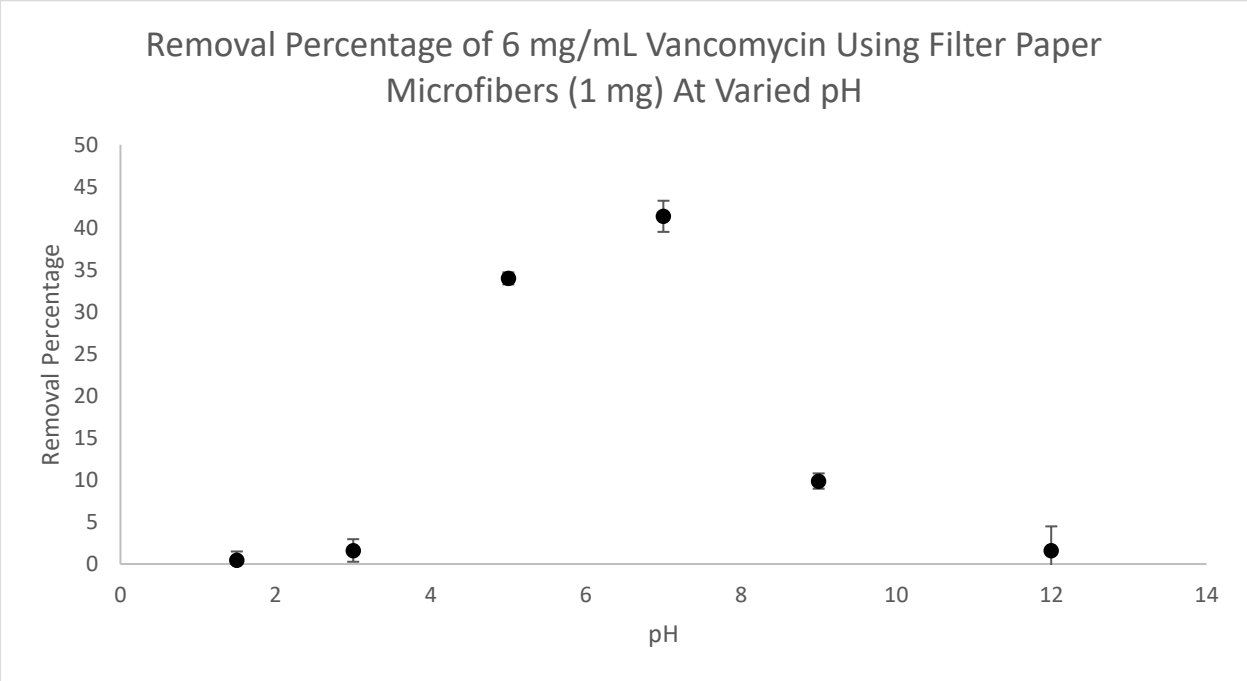

Figure 31: Removal Capacity of Vancomycin (6 mg/mL) Using Filter Paper Microfibrous Precipitate (1 mg) at pH Values of 1.5, 3, 5, 7, 9, and 12

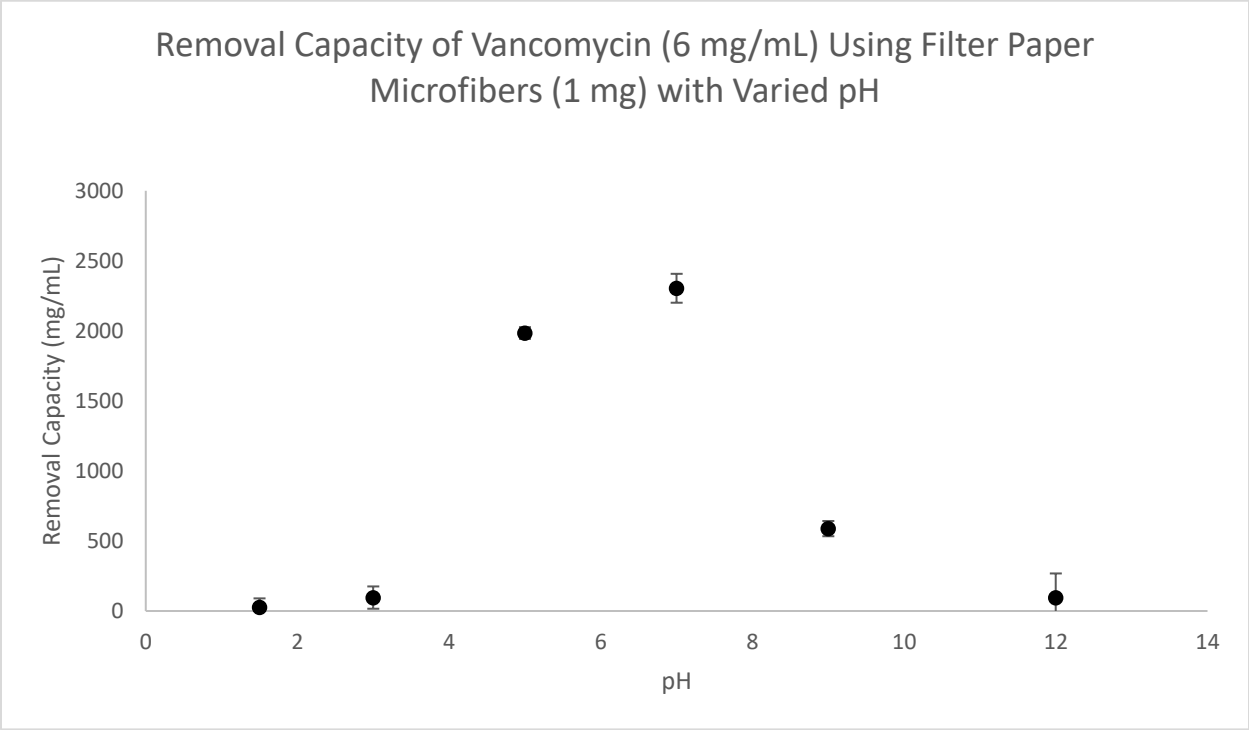

Figure 32: Removal Percentage of Vancomycin (6 mg/mL) Using Filter Paper Microfibrous Precipitate at pH Values of 1.5, 3, 5, 7, 9, and 12

The calibration curve, which was acquired in the neutral range, was not applicable to pH ranges that exceeded this neutral ragne, since the protonation states of vancomycin at low and high pH changed the electronics of the structure such that the absorbance was more pronounced or less pronounced. As such, for the data points at pH 1.5, 3, 9, and 12, the concentrations were acquired by acidifying 500 µL of the supernatants of each solution to a neutral pH such that it matched up with the calibration curve. The additional volume of acid or base added to achieve a neutral pH was accounted for to back-calculate the equilibrium concentration of each centrifuge tube.

The low removal percentage not exceeding 50% was expected due to the fact that an excess of antibiotic was introduced, 6 mg/mL for 1 mg of adsorbent. This experimental design was rationalized to be in the saturation region of the adsorption isotherm to ensure that for all

trials, the excess of antibiotics was maintained. Importantly, the removal capacity at pH 7 was found to be almost identical to the maximum removal capacity seen previously at pH 6.5. At pH 7, the removal capacity was shown to be 2304 $\pm$ 103 mg/g, which was slightly greater than the 2116 $\pm$ 29 mg/g found at pH 6.5. These two values are expected to be very near each other, due to the fact that their conditions are almost identical. However, it also proves that pH 7 is slightly better for removal than pH 6.5, which makes sense since at this pH the amine of vancomycin is still protonated while the carboxylic acids of the celluloses are more deprotonated, thus maximizing the electrostatic interaction at pH 7, even more so than at a pH value of 6.5

The trends shown in **Figure 31** and **Figure 32** match the anticipated trends based on literature pKa values. At low pH below 5 and high pH values above 9, removal is found to be extremely low. This reaffirms the idea that electrostatic interaction is responsible for removal since the best removal occurs in the range where both the vancomycin is positively charged and the cellulose filter paper precipitate is negatively charged. The trend represented in the removal capacities and percentages is reaffirmed by analyzing the precipitate levels seen in each sample. Clearly, from **Figure 33,** pH 5 and 7 have the most significant precipitate amount, followed then by pH 3 and pH 9, with pH values of 1.5 and 12 having the lowest precipitation amounts and

also corresponding to the conditions with the least removal.

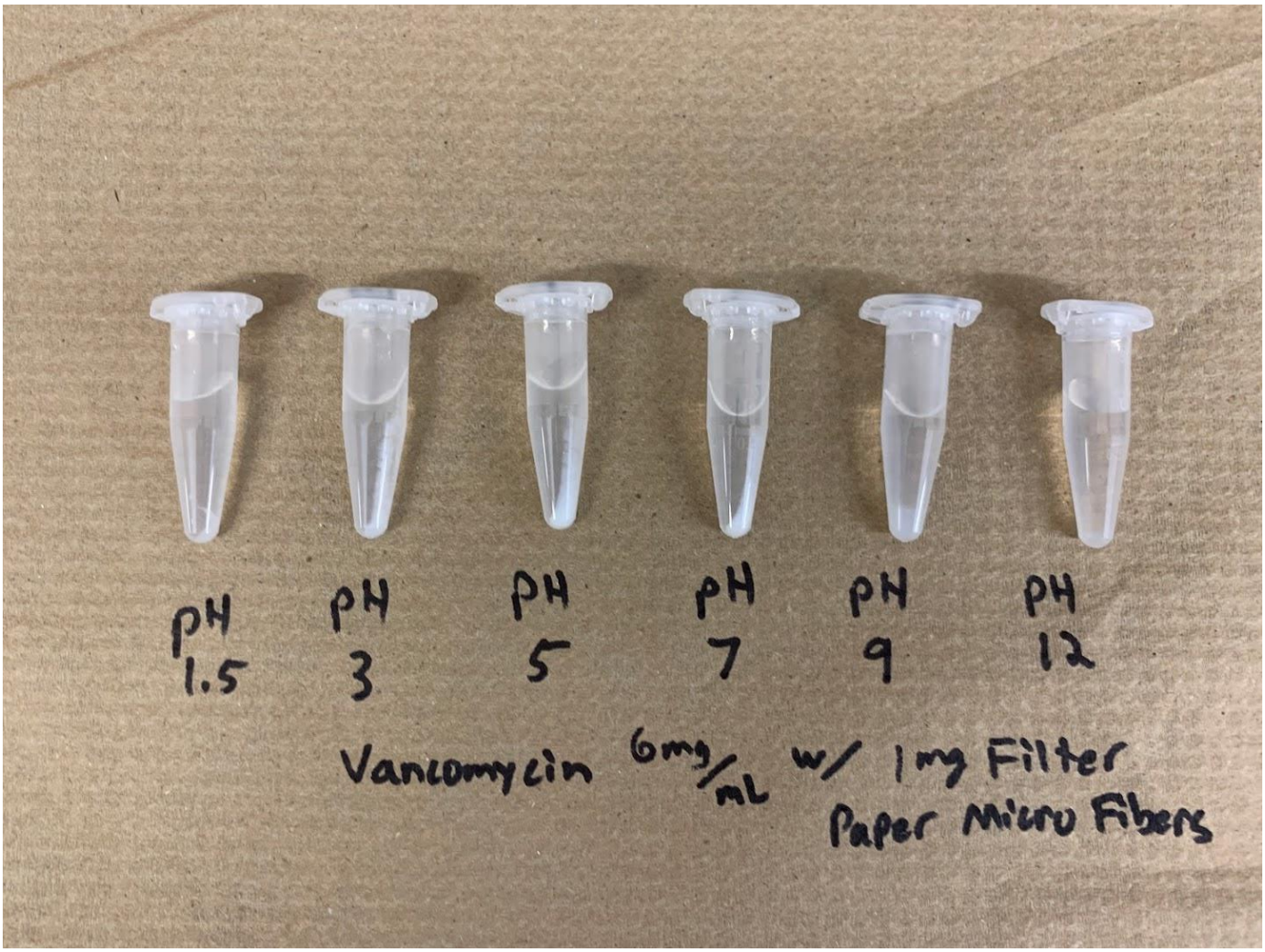

Figure 33: Visual Precipitation Amounts of Vancomycin (6 mg/mL) Removed with 1 mg of Filter Paper Microfibers

The amount of precipitate directly correlates to the removal ability at those conditions because the assessment of the concentration is performed on the supernatant, while the adsorbent takes the vancomycin out of solution, as seen visually accumulating more precipitate when more vancomycin is taken out of solution. This mechanism is directly applicable to larger scale wastewater treatment because flocculation is a common method of removal of contaminants,

whereby a “floc” is formed of the adsorbed contaminants, allowing for phase separation of the contaminants from the solution as the supernatant is now rid of them.[88]

IV. Ionic Strength Comparison

A final test of the efficacy of an adsorbent for further application is to determine its selectivity and ability to work despite other targets being present in solution. Both in wastewater treatment and in the body, antibiotics are far from the only species present, and so achieving some level of selectivity when seeking to remove the antibiotic is critical. Since this method of vancomycin removal has been shown to be through electrostatic interactions between the negatively charged carboxylated microfibers and the positively charged vancomycin at physiological pH 6.5, the impact that the presence of other ions has on removal ability is extremely important. In the body, sodium and calcium are extremely common ions to be found in their monovalent and divalent cationic species respectively, and as such, these cations are great competitors for testing the effect of ionic strength on the removal ability.[89] Testing cations is important since the anionic filter paper microfibers will interact with cations through, presumably, the same mechanism through which they interact with the cationic vancomycin, and so the presence of competing ions will show how robust this adsorbent is. The concentrations of Na^+ and Ca^{2+} in the serum for typical healthy humans are roughly 140 mmol/L and 1.4 mmol/L respectively, where a mmol/L is equivalent to a mM.[90,91]

Due to the relevance of assessing ionic strength’s impact on removal, this experiment will test the relative removal ability of vancomycin (6 mg/mL) in the presence of each ion, up to the physiologically relevant range at pH 6.5. Thus, the upper set point for amount of each ion

concentration was set to just above the physiological upper end of blood concentration, using 150 mM for Na^+ and 1.5 mM for Ca^{2+} as the maximum concentrations and testing 0, 50, 100, and 150 mM Na^+ and 0, 0.5, 1.0, and 1.5 mM Ca^{2+}. The removal capacity and percentage at each of these salt concentrations using 1 mg/mL of carboxylated cellulose filter paper microfibers at pH 6.5 were recorded in **Figures 34, 35, 36,** and **37**.

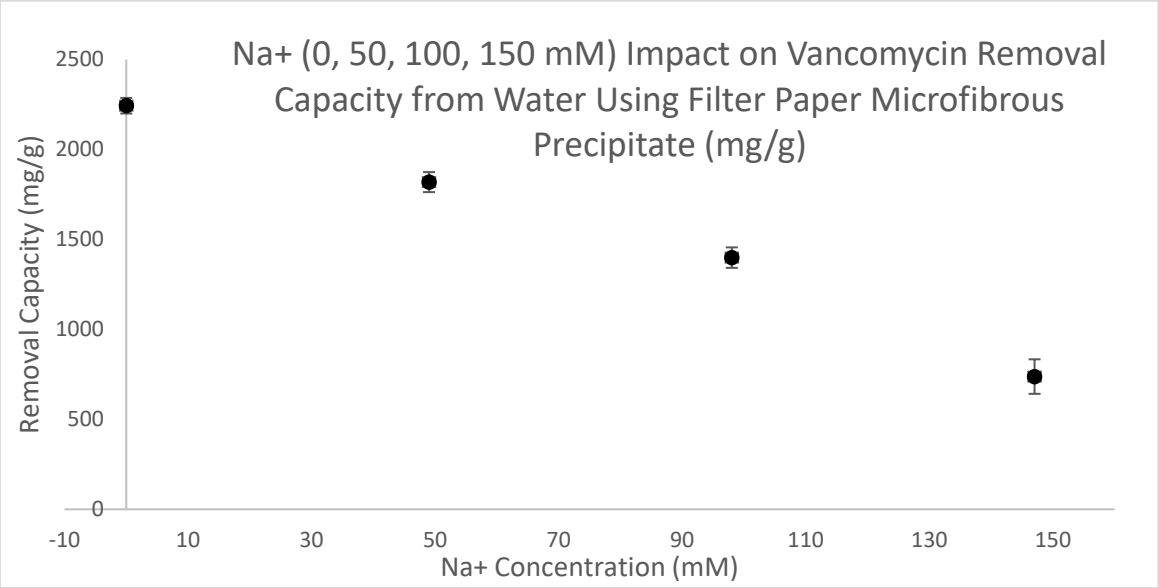

Figure 34: Impact of Na+ Concentration on Removal Capacity of Vancomycin Using Filter Paper Microfibrous Precipitate

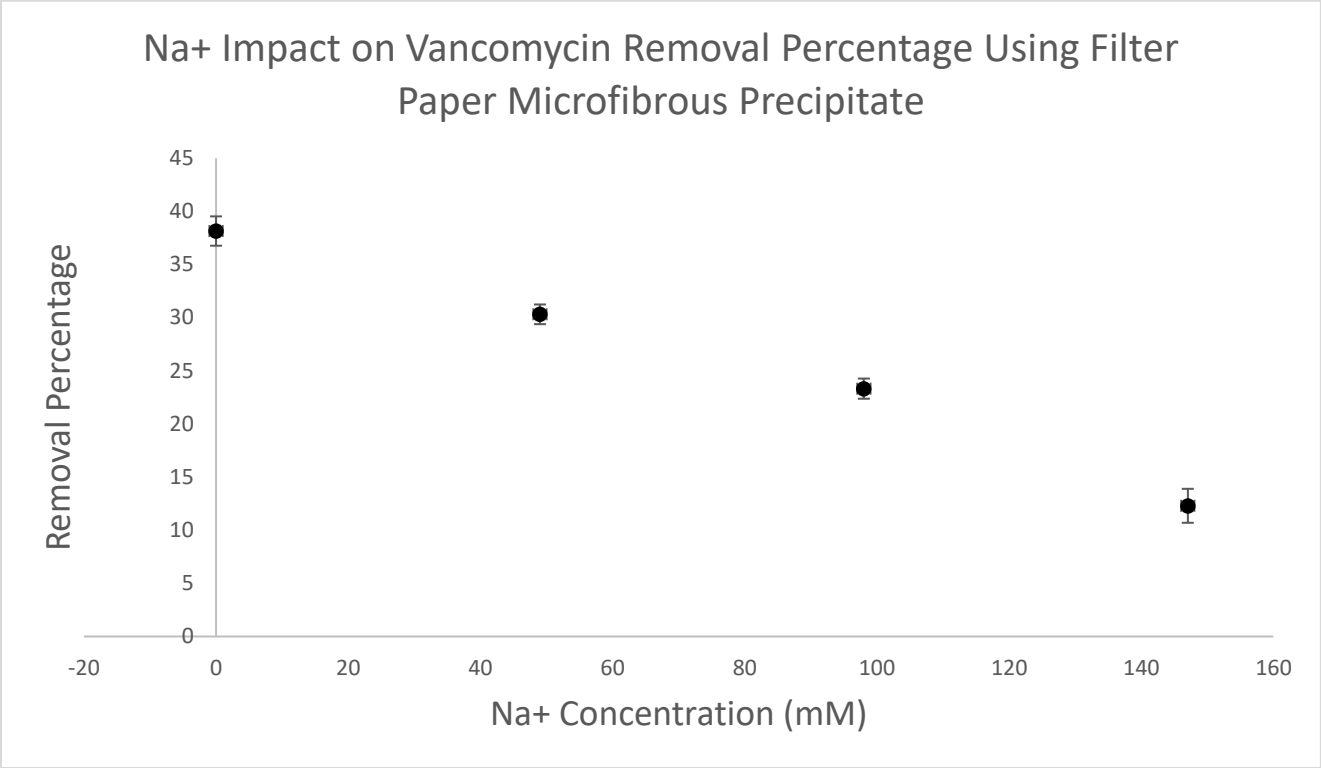

Figure 35: Na+ Concentration Impact on Vancomycin Removal Percentage from Water Using 1mg/mL Filter Paper Microfibrous Precipitate

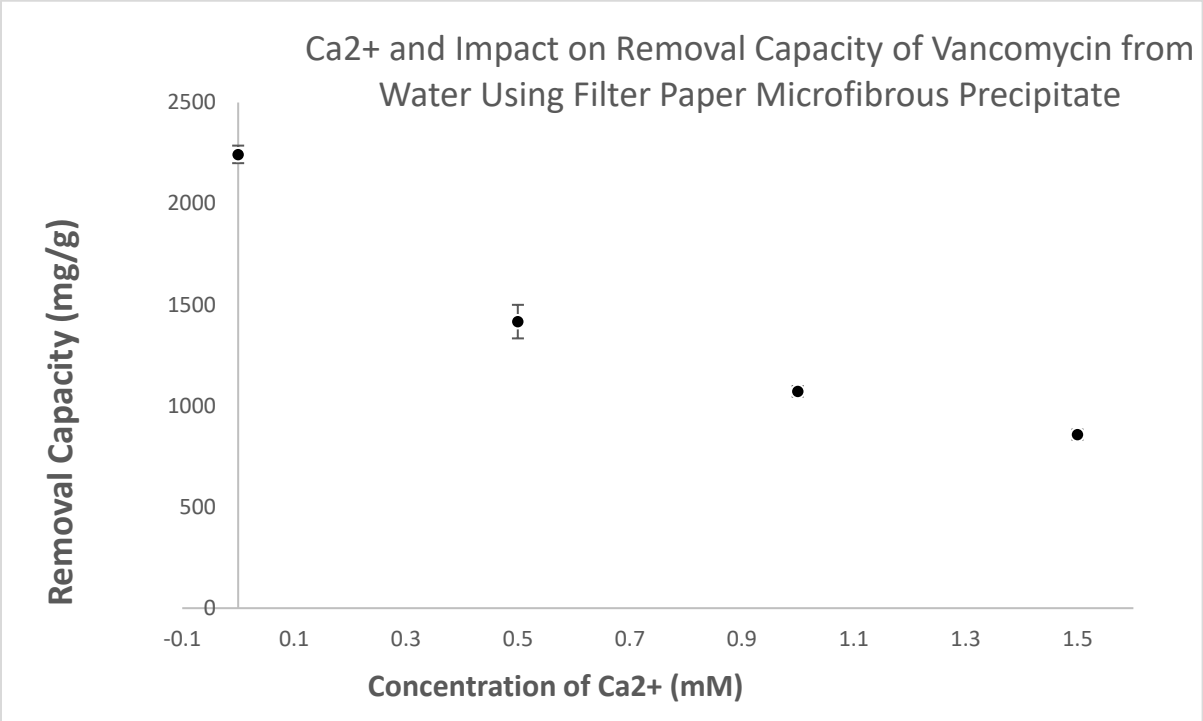

Figure 36: Ca2+ Impact on Removal Capacity of Vancomycin (6 mg/mL) Using Filter Paper Microfibrous Precipitate (1 mg/mL) at pH 6.5

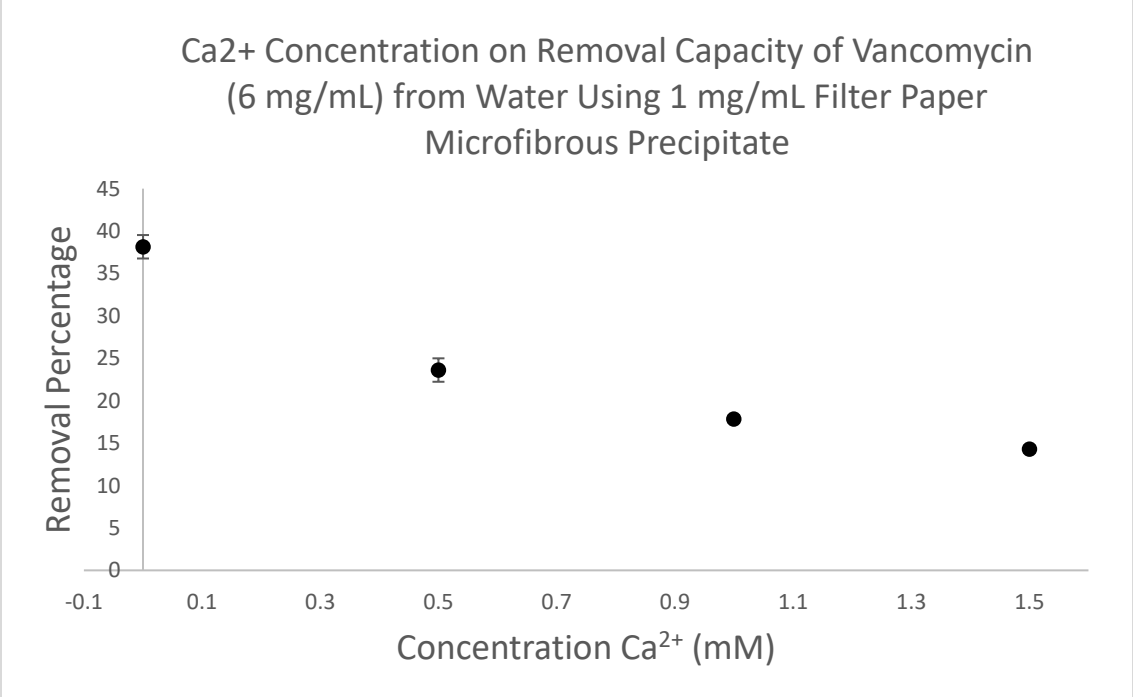

Figure 37: Impact of Ca2+ Concentration on Removal Percentage of Vancomycin (6 mg/mL) from Water Using 1 mg/mL Filter Paper Microfibrous Precipitate

Importantly, the trial with no salt returns the expected removal capacity of 2200 mg/g seen previously, serving as a control for the salt competition experiments. As expected, for calcium, the addition of competitive calcium cations decreased the removal capacity. However, it was expected that the sodium ions would merely screen charge and not hinder removal, which is not what occurred, meaning further research is necessary to investigate the sodium ion interference with removal. Notably, and importantly for the implementation of this adsorbate physiologically, the removal capacity at physiological Na^+ and Ca^{2+} concentrations (150 mM and 1.5 mM respectively) remained non-zero. Referring back to **Table 4** comparing the reported removal capacities for different adsorbents for vancomycin removal from water, the highest reported removal capacity for vancomycin in literature is 861 mg/g. Even in these disadvantaged conditions of competing salt content, the sodium trial was able to retain 738 mg/g removal while the calcium trial retained 858 mg/g removal of vancomycin, demonstrating that the carboxylated cellulose filter paper microfibrous precipitate is an extremely robust adsorbent that will be able to withstand the selectivity issues associated with competing salts in the body.

The data in **Figures 30** through **33** show the expected incremental drops in removal capacity associated with increased salt content. Simply, as the competing cation concentration increases by the same margin, saturating sites on the anionic carboxylates on the cellulose by that margin, the removal ability of the cellulose will also decrease incrementally, which is why the removal capacities drop nearly linearly with salt concentration.

II. Linezolid

Linezolid is another extremely important antibiotic of last resort, and as such, its removal is crucial.[92] However, whether it be due to its novelty or its difficulty to remove due to its uncharged nature, there is no reported literature removal capacities for any materials functionalized for the removal of linezolid from water, contributing to the novelty of this work. The most important type of removal for antibiotics is the ability to remove low concentrations since these compounds are only present in μg/mL concentration, and so achieving removal below 1 mg/mL is crucial for both wastewater treatment and medicinal applications. Despite its high charge content, ENCC has been shown to be limited in its ability to precipitate low concentrations of antibiotics from solution. This idea was proven in **Figure 38** to show that ENCC was unable to effectively remove linezolid completely, even when linezolid concentration is initially low.

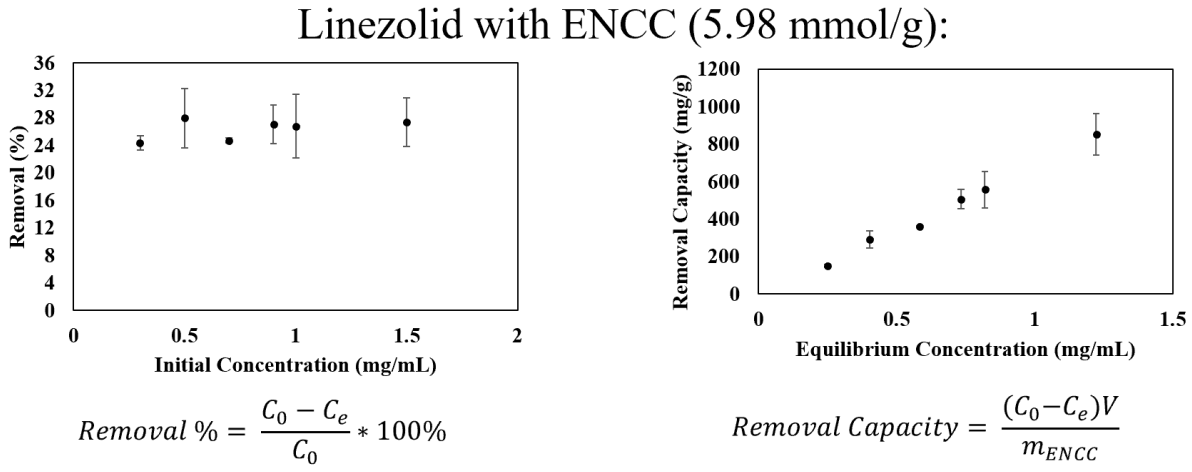

Figure 38: Linezolid Removal with ENCC. Removal percentage is plotted versus initial concentration of linezolid (mg/mL) while removal capacity is plotted with equilibrium concentration (mg/mL).

The removal percentage stagnated at approximately 30%, with a maximum removal capacity of approximately 850 mg/g. While this development is impressive considering no groups have shown removal of linezolid from water, it is especially concerning considering the very low removal capacities at low concentrations of linezolid antibiotics, where it matters most. Removing only 30% of linezolid is far from impressive, and will not prevent much off-target antibiotic resistance, so it is crucial to achieve better removal abilities at these low concentrations.

To test the hypothesis that due to the larger size of the microfibers, while still containing carboxylate groups to potentially cause interactions with linezolid or form hydrogen bonds due to the uncharged nature of linezolid, the filter paper microfibrous precipitate was used to attempt to remove linezolid from solution. The experiment was carried out at a physiological pH of 6.5 to be relevant data towards removal of excess linezolid from the body. Experiments of concentrations of 0.025 mg/mL, 0.125 mg/mL, 0.4375 mg/mL, 0.96 mg/mL, 1.25 mg/mL of linezolid were attempted to be removed using 1 mg of Microfibrous precipitate from filter paper in 1 mL total volume samples. The 0.76 mg/mL of vancomycin represents a one-to-one stoichiometric ratio of linezolid to carboxylate to sample at ratios with excess filter paper carboxylate and excess linezolid. However, very low removal was experienced using the carboxylated cellulose filter paper microfibers at any of these concentrations, with removal

capacities of nominally zero as seen in **Figure 39** with **Figure 40** showing the low removal percentages for each concentration tested.

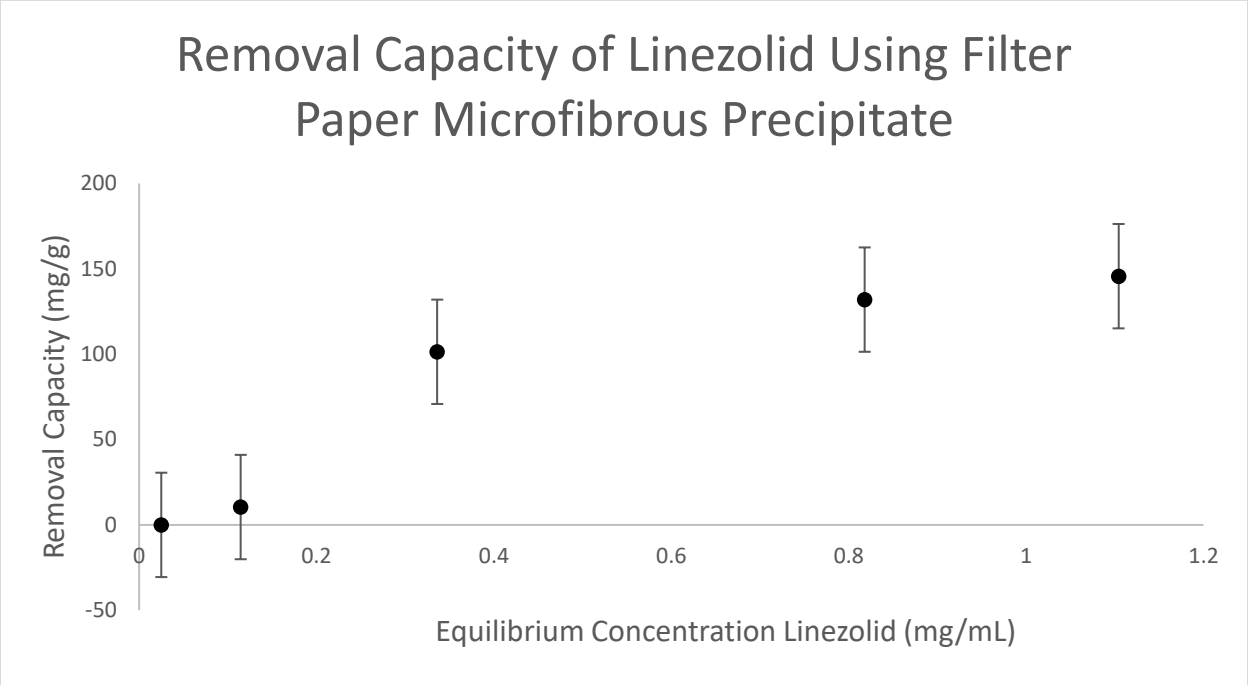

Figure 39: Removal Capacity of Linezolid (0.025 mg/mL, 0.125 mg/mL, 0.4375 mg/mL, 0.96 mg/mL, 1.25 mg/mL) Using Filter Paper Microfibrous Precipitate

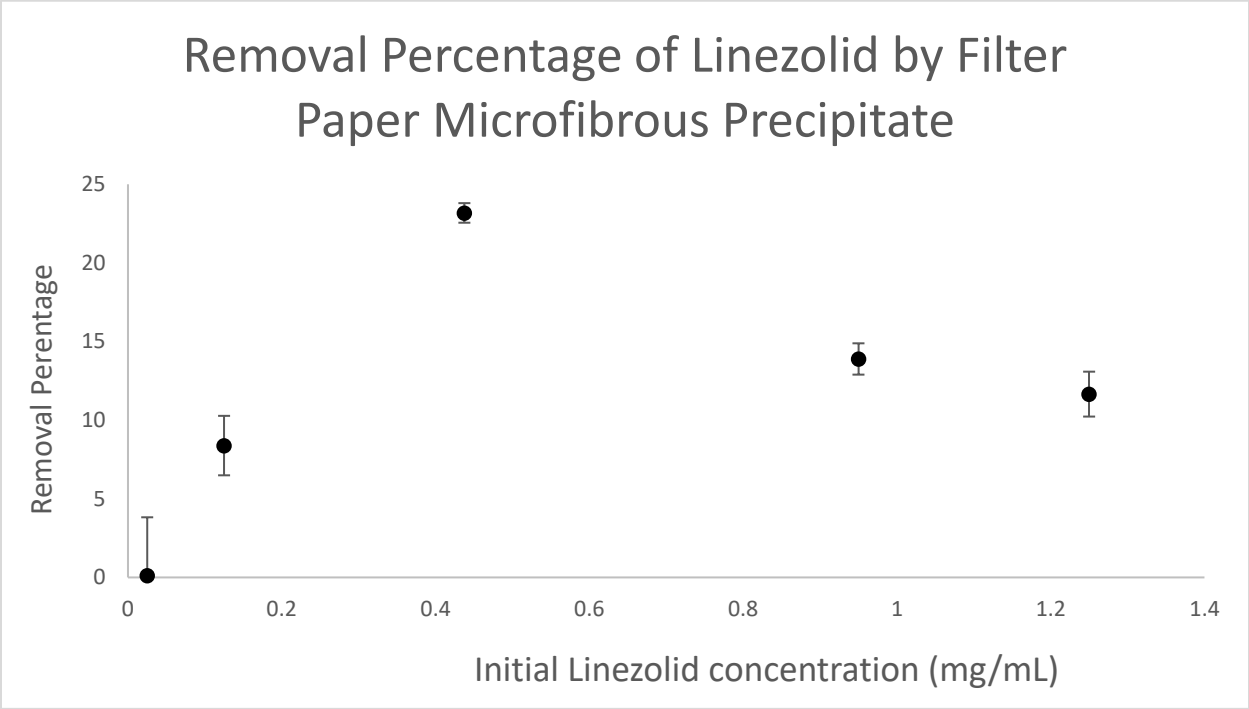

Figure 40: Removal Percentage of Linezolid Using Filter Paper Carboxylated Microfibrous Precipitate

The error bars for the removal capacity appear very large due to the overall low removal capacity, but overall, this experiment shows that ENCC remains a superior

Interestingly, the ENCC was able to have low, but still non-zero removal of linezolid, and achieve 30% removal for each sample, as shown in **Figure 38**. However, the other carboxylated cellulose adsorbent, the filter paper microfibers, was unable to remove any linezolid despite its larger size and phase separation that was anticipated to be advantageous for removing lower concentrations through precipitation. The removal percentage is an important consideration though, and showed that the microfibrous precipitate of filter paper was able to remove up to 25% of the linezolid, which is encouraging moving forward for using more of the adsorbent to remove linezolid, but in general, carboxylated adsorbents seem inefficient for removal of linezolid.

Conclusion

The growing antibiotic resistance crisis is one that, without change in current prescription habits or drastic change in the way we remove excess antibiotics from our bodies and water supply, will continue to grow and soon render society without a potent weapon against a broad spectrum of diseases.[93] The adsorption of antibiotics from either wastewater or directly from the serum is a desirable method in decreasing antibiotic contact with cells and as a result, diminishing the effects and rate of antibiotic resistance evolution. Considering cellulose is the most widely available biopolymer in the world, and is a green and inexpensive source to functionalize for widespread applications from laminates to adsorbents, it is a great option to use as a backbone for antibiotic removal. Numerous adsorbents have already been synthesized using cellulose by imparting different charged functionalities on its backbone, such as carboxylated hairy nanocelluloses (ENCC) for copper (II) removal.[61] As a result, this work focused on making use of a well-documented cellulose functionalization reaction scheme or first periodate oxidation to DAMC followed by chlorite oxidation to carboxylated nanocelluloses, but instead of focusing on the nanocellulose (ENCC) product, using the previously considered byproduct, the carboxylated microfibrous precipitate.

Two cellulose sources were tested for their abilities as an adsorbent of vancomycin: Whatman filter paper and Softwood Kraft Pulp. Despite the sequential periodate-chlorite oxidation yielding more densely carboxylated Softwood Kraft Pulp (4.22 mmol/g) compared to Whatman Filter Paper (2.26 mmol/g), it was found that the Whatman Filter Paper microfibrous precipitate was far more effective at removing vancomycin from aqueous solution at pH 6.5, achieving a removal capacity of 2116 mg/g compared to 768 mg/g for the Softwood Kraft Pulp product. The reasoning behind why the lower carboxylated product as more effective at

removing vancomycin despite the mechanism being electrostatic interaction has yet to be elucidated and requires future research.

The removal of numerous concentrations of vancomycin from solution using Whatman Filter Paper carboxylated microfibrous precipitate were tested and compiled to show a plateau of removal capacity at approximately 2200 mg/g, a significant improvement over the other reported adsorbents in the literature, which have not exceed a removal capacity of 861 mg/g.[75] To elucidate the mechanism of vancomycin removal, the removal ability of this adsorbent was tested at pH 1.5, 3, 5, 7, 9, and 12, to show that removal peaked at pH 7 with a removal capacity of 2300 mg/g while it dropped significantly outside of the 5 to 7 range, where either vancomycin was deprotonated and neutrally charged or the carboxylated microfibrous precipitate was fully protonated and neutrally charged, or both, which indicated that electrostatic interaction was responsible for removal. Additionally, this mechanism was confirmed by demonstrating that the uncharged starting material to make the carboxylated cellulose microfibrous precipitate of filter paper, DAMC, was unable to remove any vancomycin. Upon fitting the data to the Langmuir model, it was found to fit very well, indicating that the adsorption of vancomycin from aqueous solution occurs as a monolayer with low adsorbate-adsorbate interactions.

To evaluate the impact that competing cations had on removal capacity for this adsorbent, removal trials were performed in the presence of Na^+ and Ca^{2+} to find that the presence of both ions independently and incrementally decreased the removal ability of the microfibrous precipitate. This trend was unexpected for the sodium ion, since unlike calcium, it is not known to aggregate colloidal systems.[94] However, importantly, in the presence of physiological Na^+ and Ca^{2+} concentrations of 150 mM and 1.5 mM respectively, the removal capacity still exceeded

700 mg/g, at 737 and 858 mg/g respectively, indicating that despite this hindering, exceptional removal of vancomycin could still be achieved in the body.

Finally, the removal of another important antibiotic of last resort, linezolid, was tested to analyze the ability of the filter paper microfibrous precipitate to remove a neutrally charged species. It was found, however, that while ENCC could successfully remove at least 30% of linezolid in solution to achieve a removal capacity of approximately 850 mg/g, the microfibrous precipitate was unable to remove virtually any of the linezolid, proving in both cases, that to achieve effective removal of this antibiotic, better materials must be synthesized to target this neutrally charged linezolid molecule.

The carboxylated cellulose microfibrous precipitate, specifically of Whatman Filter Paper has proven to be an effective adsorbent for the cationic antibiotic of last resort, vancomycin. Its existence as a microfiber that is already phase separated, as proven by light microscopy and its precipitation from water, is advantageous for application in removing lower, more relevant concentrations of antibiotics from water. Further investigation into the widespread applications of this adsorbent is necessary, but this work has illustrated how even modestly charged (2.26 mmol/g) microfibers that were previously considered a byproduct of chlorite oxidation of DAMC have potential in expanded applications in combatting the antibiotic resistance crisis.

BIBLIOGRAPHY

(1) Richardson, S. D.; Ternes, T. A. Water Analysis: Emerging Contaminants and Current Issues. *Anal. Chem.* **2014**, *86* (6), 2813–2848. https://doi.org/10.1021/ac500508t.

(2) Tan, S. Y.; Tatsumura, Y. Alexander Fleming (1881-1955): Discoverer of Penicillin. *Singapore Med. J.* **2015**, *56* (7), 366–367. https://doi.org/10.11622/smedj.2015105.

(3) Bennett, J. W.; Chung, K.-T. B. T.-A. in A. M. Alexander Fleming and the Discovery of Penicillin; Academic Press, 2001; Vol. 49, pp 163–184. https://doi.org/https://doi.org/10.1016/S0065-2164(01)49013-7.

(4) Davies, J. Where Have All the Antibiotics Gone? *Can. J. Infect. Dis. Med. Microbiol. = J. Can. des Mal. Infect. la Microbiol. medicale* **2006**, *17* (5), 287–290. https://doi.org/10.1155/2006/707296.

(5) Adedeji, W. A. THE TREASURE CALLED ANTIBIOTICS. *Ann. Ibadan Postgrad. Med.* **2016**, *14* (2), 56–57.

(6) Silver, L. L. Challenges of Antibacterial Discovery. *Clin. Microbiol. Rev.* **2011**, *24* (1), 71–109. https://doi.org/10.1128/CMR.00030-10.

(7) Huddleston, J. R. Horizontal Gene Transfer in the Human Gastrointestinal Tract: Potential Spread of Antibiotic Resistance Genes. *Infect. Drug Resist.* **2014**, *7*, 167–176. https://doi.org/10.2147/IDR.S48820.

(8) Editors, P. M. Antimicrobial Resistance: Is the World UNprepared? *PLoS Med.* **2016**, *13* (9), e1002130–e1002130. https://doi.org/10.1371/journal.pmed.1002130.

(9) De Clercq, E. Antivirals and Antiviral Strategies. *Nat. Rev. Microbiol.* **2004**, *2* (9), 704–720. https://doi.org/10.1038/nrmicro975.

(10) Wise, R. A Review of the Mechanisms of Action and Resistance of Antimicrobial Agents. *Can. Respir. J.* **1999**, *6 Suppl A*, 20A-2A.

(11) Džidić, S.; Šušković, J.; Kos, B. Antibiotic Resistance Mechanisms in Bacteria: Biochemical and Genetic Aspects. *Food Technol. Biotechnol.* **2008**, *46* (1).

(12) Grundmann, H.; Aires-de-Sousa, M.; Boyce, J.; Tiemersma, E. Emergence and Resurgence of Meticillin-Resistant Staphylococcus Aureus as a Public-Health Threat. *Lancet (London, England)* **2006**, *368* (9538), 874–885. https://doi.org/10.1016/S0140-6736(06)68853-3.

(13) Miller, W. R.; Bayer, A. S.; Arias, C. A. Mechanism of Action and Resistance to Daptomycin in Staphylococcus Aureus and Enterococci. *Cold Spring Harb. Perspect. Med.* **2016**, *6* (11), a026997. https://doi.org/10.1101/cshperspect.a026997.

(14) Bozdogan, B.; Appelbaum, P. C. Oxazolidinones: Activity, Mode of Action, and Mechanism of Resistance. *Int. J. Antimicrob. Agents* **2004**, *23* (2), 113–119. https://doi.org/10.1016/j.ijantimicag.2003.11.003.

(15) Davies, J.; Davies, D. Origins and Evolution of Antibiotic Resistance. *Microbiol. Mol. Biol. Rev.* **2010**, *74* (3), 417–433. https://doi.org/10.1128/MMBR.00016-10.

(16) Hacker, J.; Kaper, J. B. Pathogenicity Islands and the Evolution of Microbes. *Annu. Rev. Microbiol.* **2000**, *54*, 641–679. https://doi.org/10.1146/annurev.micro.54.1.641.

(17) Martínez, J. L.; Coque, T. M.; Lanza, V. F.; de la Cruz, F.; Baquero, F. Genomic and Metagenomic Technologies to Explore the Antibiotic Resistance Mobilome. *Ann. N. Y. Acad. Sci.* **2017**, *1388* (1), 26–41. https://doi.org/10.1111/nyas.13282.

(18) Berkner, S.; Konradi, S.; Schönfeld, J. Antibiotic Resistance and the Environment--There and Back Again: Science & Society Series on Science and Drugs. *EMBO Rep.* **2014**, *15*

(7), 740–744. https://doi.org/10.15252/embr.201438978.
(19) Polesel, F.; Andersen, H. R.; Trapp, S.; Plósz, B. G. Removal of Antibiotics in Biological Wastewater Treatment Systems—A Critical Assessment Using the Activated Sludge Modeling Framework for Xenobiotics (ASM-X). *Environ. Sci. Technol.* **2016**, *50* (19), 10316–10334. https://doi.org/10.1021/acs.est.6b01899.
(20) Milani, R. V; Wilt, J. K.; Entwisle, J.; Hand, J.; Cazabon, P.; Bohan, J. G. Reducing Inappropriate Outpatient Antibiotic Prescribing: Normative Comparison Using Unblinded Provider Reports. *BMJ open Qual.* **2019**, *8* (1), e000351–e000351. https://doi.org/10.1136/bmjoq-2018-000351.
(21) FDA. Summary Report On Antimicrobials Sold or Distributed for Use in Food-Producing Animals. **2014**.
(22) Sarmah, A. K.; Meyer, M. T.; Boxall, A. B. A. A Global Perspective on the Use, Sales, Exposure Pathways, Occurrence, Fate and Effects of Veterinary Antibiotics (VAs) in the Environment. *Chemosphere* **2006**, *65* (5), 725–759. https://doi.org/10.1016/j.chemosphere.2006.03.026.
(23) Rodríguez-Molina, D.; Mang, P.; Schmitt, H.; Chifiriuc, M. C.; Radon, K.; Wengenroth, L. Do Wastewater Treatment Plants Increase Antibiotic Resistant Bacteria or Genes in the Environment? Protocol for a Systematic Review. *Syst. Rev.* **2019**, *8* (1), 304. https://doi.org/10.1186/s13643-019-1236-9.
(24) Su, R.; Zhang, G.; Wang, P.; Li, S.; Ravenelle, R. M.; Crittenden, J. C. Treatment of Antibiotic Pharmaceutical Wastewater Using a Rotating Biological Contactor. *J. Chem.* **2015**, *2015*, 705275. https://doi.org/10.1155/2015/705275.
(25) Sengupta, S.; Chattopadhyay, M. K.; Grossart, H.-P. The Multifaceted Roles of Antibiotics and Antibiotic Resistance in Nature. *Front. Microbiol.* **2013**, *4*, 47.
(26) Spellberg, B.; Gilbert, D. N. The Future of Antibiotics and Resistance: A Tribute to a Career of Leadership by John Bartlett. *Clin. Infect. Dis.* **2014**, *59* (suppl_2), S71–S75.
(27) Lowy, F. D. Antimicrobial Resistance: The Example of Staphylococcus Aureus. *J. Clin. Invest.* **2003**, *111* (9), 1265–1273. https://doi.org/10.1172/JCI18535.
(28) Skinner, D.; Keefer, C. S. Significance of Bacteremia Caused by Staphylococcus Aureus: A Study of One Hundred and Twenty-Two Cases and a Review of the Literature Concerned with Experimental Infection in Animals. *Arch. Intern. Med.* **1941**, *68* (5), 851–875.
(29) Ventola, C. L. The Antibiotic Resistance Crisis: Part 1: Causes and Threats. *P T* **2015**, *40* (4), 277–283.
(30) Yoshikawa, T. T. Antimicrobial Resistance and Aging: Beginning of the End of the Antibiotic Era? *J. Am. Geriatr. Soc.* **2002**, *50*, 226–229.
(31) Niki, Y. [Practical guidelines for the management and treatment of infections caused by MRSA, the 2nd Edition]. *Kansenshogaku zasshi. J. Japanese Assoc. Infect. Dis.* **2014**, *88* (5), 597–668.
(32) Conly, J.; Johnston, B. Where Are All the New Antibiotics? The New Antibiotic Paradox. *Can. J. Infect. Dis. Med. Microbiol. = J. Can. des Mal. Infect. la Microbiol. medicale* **2005**, *16* (3), 159–160. https://doi.org/10.1155/2005/892058.
(33) Howden, B. P.; Davies, J. K.; Johnson, P. D. R.; Stinear, T. P.; Grayson, M. L. Reduced Vancomycin Susceptibility in Staphylococcus Aureus, Including Vancomycin-Intermediate and Heterogeneous Vancomycin-Intermediate Strains: Resistance Mechanisms, Laboratory Detection, and Clinical Implications. *Clin. Microbiol. Rev.* **2010**,

23 (1), 99–139.

(34) Hasan, R.; Acharjee, M.; Noor, R. Prevalence of Vancomycin Resistant Staphylococcus Aureus (VRSA) in Methicillin Resistant S. Aureus (MRSA) Strains Isolated from Burn Wound Infections. *Ci ji yi xue za zhi = Tzu-chi Med. J.* **2016**, *28* (2), 49–53. https://doi.org/10.1016/j.tcmj.2016.03.002.

(35) ASHRAFUL HAQ, J.; MUSHFEQUR RAHMAN, M.; ZAHURUL HAQUE ASNA, S. M.; AKRAM HOSSAIN, M.; Ahmed, I. Methicillin-Resistant Staphylococcus Aureus in Bangladesh: A Multicentre Study. *Int. J. Antimicrob. Agents* **2005**, *25* (3), 276–277.

(36) Jones, R. N.; Fritsche, T. R.; Sader, H. S.; Ross, J. E. LEADER Surveillance Program Results for 2006: An Activity and Spectrum Analysis of Linezolid Using Clinical Isolates from the United States (50 Medical Centers). *Diagn. Microbiol. Infect. Dis.* **2007**, *59* (3), 309–317.

(37) Davis, S. L.; McKinnon, P. S.; Hall, L. M.; Delgado Jr, G.; Rose, W.; Wilson, R. F.; Rybak, M. J. Daptomycin versus Vancomycin for Complicated Skin and Skin Structure Infections: Clinical and Economic Outcomes. *Pharmacother. J. Hum. Pharmacol. Drug Ther.* **2007**, *27* (12), 1611–1618.

(38) Kulkarni, P.; Olson, N. D.; Raspanti, G. A.; Rosenberg Goldstein, R. E.; Gibbs, S. G.; Sapkota, A.; Sapkota, A. R. Antibiotic Concentrations Decrease during Wastewater Treatment but Persist at Low Levels in Reclaimed Water. *Int. J. Environ. Res. Public Health* **2017**, *14* (6), 668. https://doi.org/10.3390/ijerph14060668.

(39) Goldstein, R. E. R.; Micallef, S. A.; Gibbs, S. G.; George, A.; Claye, E.; Sapkota, A.; Joseph, S. W.; Sapkota, A. R. Detection of Vancomycin-Resistant Enterococci (VRE) at Four US Wastewater Treatment Plants That Provide Effluent for Reuse. *Sci. Total Environ.* **2014**, *466*, 404–411.

(40) de Souza Lima, M. M.; Borsali, R. Rodlike Cellulose Microcrystals: Structure, Properties, and Applications. *Macromol. Rapid Commun.* **2004**, *25* (7), 771–787. https://doi.org/10.1002/marc.200300268.

(41) Habibi, Y.; Lucia, L. A.; Rojas, O. J. Cellulose Nanocrystals: Chemistry, Self-Assembly, and Applications. *Chem. Rev.* **2010**, *110* (6), 3479–3500. https://doi.org/10.1021/cr900339w.

(42) Hosemann, R. Crystallinity in High Polymers, Especially Fibres. *Polymer (Guildf).* **1962**, *3*, 349–392.

(43) Chen, D.; van de Ven, T. G. M. Morphological Changes of Sterically Stabilized Nanocrystalline Cellulose after Periodate Oxidation. *Cellulose* **2016**, *23* (2), 1051–1059. https://doi.org/10.1007/s10570-016-0862-9.

(44) Klemm, D.; Kramer, F.; Moritz, S.; Lindström, T.; Ankerfors, M.; Gray, D.; Dorris, A. Nanocelluloses: A New Family of Nature-Based Materials. *Angew. Chemie Int. Ed.* **2011**, *50* (24), 5438–5466. https://doi.org/https://doi.org/10.1002/anie.201001273.

(45) Kalia, S.; Dufresne, A.; Cherian, B. M.; Kaith, B. S.; Avérous, L.; Njuguna, J.; Nassiopoulos, E. Cellulose-Based Bio- and Nanocomposites: A Review. *Int. J. Polym. Sci.* **2011**, *2011*, 837875. https://doi.org/10.1155/2011/837875.

(46) AU - Sheikhi, A.; AU - Yang, H.; AU - Alam, M. N.; AU - van de Ven, T. G. M. Highly Stable, Functional Hairy Nanoparticles and Biopolymers from Wood Fibers: Towards Sustainable Nanotechnology. *JoVE* **2016**, No. 113, e54133. https://doi.org/doi:10.3791/54133.

(47) Van De Ven, T. G. M.; Sheikhi, A. Hairy Cellulose Nanocrystalloids: A Novel Class of

Nanocellulose. *Nanoscale* **2016**, *8* (33), 15101–15114. https://doi.org/10.1039/c6nr01570k.
(48) Méndez-Vilas, A. Microscopy: Science, Technology, Applications and Education.
(49) Sheikhi, A.; Yang, H.; Carreau, P. J.; van de Ven, T. G. M. Colloidal Nano-Toolbox for Molecularly Regulated Polymerization: Chemorheology over 6 Decades of Viscoelasticity. *Mater. Horizons* **2017**, *4* (6), 1165–1170. https://doi.org/10.1039/C7MH00575J.
(50) Yang, H.; Chen, D.; van de Ven, T. G. M. Preparation and Characterization of Sterically Stabilized Nanocrystalline Cellulose Obtained by Periodate Oxidation of Cellulose Fibers. *Cellulose* **2015**, *22* (3), 1743–1752. https://doi.org/10.1007/s10570-015-0584-4.
(51) Hessler, L. E.; Merola, G. V; Berkley, E. E. Degree of Polymerization of Cellulose in Cotton Fibers. *Text. Res. J.* **1948**, *18* (10), 628–634. https://doi.org/10.1177/004051754801801004.
(52) Hussein, A. A.; Al-Hadedi, A. A. M.; Mahrath, A. J.; Moustafa, G. A. I.; Almalki, F. A.; Alqahtani, A.; Shityakov, S.; Algazally, M. E. Mechanistic Investigations on Pinnick Oxidation: A Density Functional Theory Study. *R. Soc. Open Sci.* **2021**, *7* (2), 191568. https://doi.org/10.1098/rsos.191568.
(53) Batmaz, R.; Mohammed, N.; Zaman, M.; Minhas, G.; Berry, R. M.; Tam, K. C. Cellulose Nanocrystals as Promising Adsorbents for the Removal of Cationic Dyes. *Cellulose* **2014**, *21* (3), 1655–1665.
(54) Herrera-Morales, J.; Morales, K.; Ramos, D.; Ortiz-Quiles, E. O.; López-Encarnación, J. M.; Nicolau, E. Examining the Use of Nanocellulose Composites for the Sorption of Contaminants of Emerging Concern: An Experimental and Computational Study. *ACS Omega* **2017**, *2* (11), 7714–7722. https://doi.org/10.1021/acsomega.7b01053.
(55) Mohammadinejad, R.; Maleki, H.; Larrañeta, E.; Fajardo, A.; Bakhshian Nik, A.; Shavandi, A.; Sheikhi, A.; Ghorbanpour, M.; Farokhi, M.; .G, P.; et al. Status and Future Scope of Plant-Based Green Hydrogels in Biomedical Engineering. **2019**, *16*, 213–246. https://doi.org/10.1016/j.apmt.2019.04.010.
(56) Schiff, H. Mittheilungen Aus Dem Universitätslaboratorium in Pisa: Eine Neue Reihe Organischer Basen. *Justus Liebigs Ann. Chem.* **1864**, *131* (1), 118–119. https://doi.org/https://doi.org/10.1002/jlac.18641310113.
(57) Yang, H.; van de Ven, T. G. M. Preparation of Hairy Cationic Nanocrystalline Cellulose. *Cellulose* **2016**, *23* (3), 1791–1801. https://doi.org/10.1007/s10570-016-0902-5.
(58) Selkälä, T.; Suopajärvi, T.; Sirviö, J. A.; Luukkonen, T.; Kinnunen, P.; de Carvalho, A. L. C. B.; Liimatainen, H. Surface Modification of Cured Inorganic Foams with Cationic Cellulose Nanocrystals and Their Use as Reactive Filter Media for Anionic Dye Removal. *ACS Appl. Mater. Interfaces* **2020**, *12* (24), 27745–27757. https://doi.org/10.1021/acsami.0c05927.
(59) Campano, C.; Lopez-Exposito, P.; Blanco, A.; Negro, C.; van de Ven, T. G. M. Hairy Cationic Nanocrystalline Cellulose as Retention Additive in Recycled Paper. *Cellulose* **2019**, *26* (10), 6275–6289. https://doi.org/10.1007/s10570-019-02494-x.
(60) Lopez-Exposito, P.; Campano, C.; van de Ven, T. G. M.; Negro, C.; Blanco, A. Microalgae Harvesting with the Novel Flocculant Hairy Cationic Nanocrystalline Cellulose. *Colloids Surfaces B Biointerfaces* **2019**, *178*, 329–336. https://doi.org/https://doi.org/10.1016/j.colsurfb.2019.03.018.
(61) Sheikhi, A.; Safari, S.; Yang, H.; van de Ven, T. G. M. Copper Removal Using

Electrosterically Stabilized Nanocrystalline Cellulose. *ACS Appl. Mater. Interfaces* **2015**, *7* (21), 11301–11308. https://doi.org/10.1021/acsami.5b01619.
(62) Tavakolian, M.; Wiebe, H.; Sadeghi, M. A.; van de Ven, T. G. M. Dye Removal Using Hairy Nanocellulose: Experimental and Theoretical Investigations. *ACS Appl. Mater. Interfaces* **2020**, *12* (4), 5040–5049. https://doi.org/10.1021/acsami.9b18679.
(63) Chen, D.; van de Ven, T. G. M. Flocculation Kinetics of Precipitated Calcium Carbonate Induced by Electrosterically Stabilized Nanocrystalline Cellulose. *Colloids Surfaces A Physicochem. Eng. Asp.* **2016**, *504*, 11–17. https://doi.org/https://doi.org/10.1016/j.colsurfa.2016.05.023.
(64) Yang, H.; Alam, M. N.; van de Ven, T. G. M. Highly Charged Nanocrystalline Cellulose and Dicarboxylated Cellulose from Periodate and Chlorite Oxidized Cellulose Fibers. *Cellulose* **2013**, *20* (4), 1865–1875. https://doi.org/10.1007/s10570-013-9966-7.
(65) Martin, J. H.; Norris, R.; Barras, M.; Roberts, J.; Morris, R.; Doogue, M.; Jones, G. R. D. Therapeutic Monitoring of Vancomycin in Adult Patients: A Consensus Review of the American Society of Health-System Pharmacists, the Infectious Diseases Society of America, and the Society Of Infectious Diseases Pharmacists. *Clin. Biochem. Rev.* **2010**, *31* (1), 21–24.
(66) Abuhasna, S.; Al Jundi, A. H. Therapeutic Drug Monitoring of Vancomycin in an Obese Patient with Renal Insufficiency. *J. Anaesthesiol. Clin. Pharmacol.* **2011**, *27* (4), 531–533. https://doi.org/10.4103/0970-9185.86601.
(67) Giebułtowicz, J.; Nałęcz-Jawecki, G.; Harnisz, M.; Kucharski, D.; Korzeniewska, E.; Płaza, G. Environmental Risk and Risk of Resistance Selection Due to Antimicrobials' Occurrence in Two Polish Wastewater Treatment Plants and Receiving Surface Water. *Molecules* **2020**, *25* (6), 1470.
(68) Gibson, L. J. The Hierarchical Structure and Mechanics of Plant Materials. *J. R. Soc. Interface* **2012**, *9* (76), 2749–2766. https://doi.org/10.1098/rsif.2012.0341.
(69) Evans, E.; Gabriel, E. F. M.; Coltro, W. K. T.; Garcia, C. D. Rational Selection of Substrates to Improve Color Intensity and Uniformity on Microfluidic Paper-Based Analytical Devices. *Analyst* **2014**, *139* (9), 2127–2132. https://doi.org/10.1039/c4an00230j.
(70) Ullmann's Encyclopedia of Industrial Chemistry. Fifth Edition. Executive Edit.: W. Gerhardts, Weinheim, Federal Republic of Germany. Sen. Edit.: Y. St. Yamamoto, Deerfield Beach, Florida, USA. Editors: L. Kaudy, J. F. Rounsaville. G. Schulz. All Weinheim . *Starch - Stärke* **1987**, *39* (10), 373. https://doi.org/https://doi.org/10.1002/star.19870391018.
(71) Bhattacharyya, D.; Hestekin, J. A.; Brushaber, P.; Cullen, L.; Bachas, L. G.; Sikdar, S. K. Novel Poly-Glutamic Acid Functionalized Microfiltration Membranes for Sorption of Heavy Metals at High Capacity. *J. Memb. Sci.* **1998**, *141* (1), 121–135. https://doi.org/https://doi.org/10.1016/S0376-7388(97)00301-3.
(72) Herrmann, D. J.; Peppard, W. J.; Ledeboer, N. A.; Theesfeld, M. L.; Weigelt, J. A.; Buechel, B. J. Linezolid for the Treatment of Drug-Resistant Infections. *Expert Rev. Anti. Infect. Ther.* **2008**, *6* (6), 825–848. https://doi.org/10.1586/14787210.6.6.825.
(73) Patiha; Heraldy, E.; Hidayat, Y.; Firdaus, M. The Langmuir Isotherm Adsorption Equation: The Monolayer Approach. *{IOP} Conf. Ser. Mater. Sci. Eng.* **2016**, *107*, 12067. https://doi.org/10.1088/1757-899x/107/1/012067.
(74) Khayyun, T. S.; Mseer, A. H. Comparison of the Experimental Results with the Langmuir

and Freundlich Models for Copper Removal on Limestone Adsorbent. *Appl. Water Sci.* **2019**, *9* (8), 170. https://doi.org/10.1007/s13201-019-1061-2.

(75) Ahmad Nor, Y.; Zhang, H.; Purwajanti, S.; Song, H.; Meka, A. K.; Wang, Y.; Mitter, N.; Mahony, D.; Yu, C. Hollow Mesoporous Carbon Nanocarriers for Vancomycin Delivery: Understanding the Structure–Release Relationship for Prolonged Antibacterial Performance. *J. Mater. Chem. B* **2016**, *4* (43), 7014–7021. https://doi.org/10.1039/C6TB01778A.

(76) Elena, V.; Torri, G.; Graziani, G.; Montanelli, A.; Valerio, A.; Melone, L. Nanostructured Cellulose Materials: Adsorption of Antibiotics onto Cellulose Fibers Functionalized with Glycidylmethacrylate for the Manufacturing of Antibacterial Fabrics. *Tech. Proc. 2012 NSTI Nanotechnol. Conf. Expo, NSTI-Nanotech 2012* **2012**, 174–177.

(77) Likozar, B.; Senica, D.; Pavko, A. Equilibrium and Kinetics of Vancomycin Adsorption on Polymeric Adsorbent. *AIChE J.* **2012**, *58* (1), 99–106. https://doi.org/10.1002/aic.12559.

(78) Giammarco, J.; Mochalin, V. N.; Haeckel, J.; Gogotsi, Y. The Adsorption of Tetracycline and Vancomycin onto Nanodiamond with Controlled Release. *J. Colloid Interface Sci.* **2016**, *468*, 253–261. https://doi.org/https://doi.org/10.1016/j.jcis.2016.01.062.

(79) YUZURIHA, K.; YAKABE, K.; NAGAI, H.; LI, S.; ZENDO, T.; ZAI, K.; KISHIMURA, A.; HASE, K.; KIM, Y.-G.; MORI, T.; et al. Protection of Gut Microbiome from Antibiotics: Development of a Vancomycin-Specific Adsorbent with High Adsorption Capacity. *Biosci. Microbiota, Food Heal.* **2020**, *39* (3), 128–136. https://doi.org/10.12938/bmfh.2020-002.

(80) Yuan, J.; Xu, J.; Niu, W.; Zhao, Q.; Yan, H.; Cheng, X.; He, B. AFFINITY ADSORBENTS WITH D-ALANINE AND D,L-ALANINE AS LIGANDS FOR VANCOMYCIN GROUP ANTIBIOTICS. *J. Liq. Chromatogr. Relat. Technol.* **2001**, *24* (17), 2635–2645. https://doi.org/10.1081/JLC-100106091.

(81) Yan, H.; Zhao, Q.; Yuan, J.; Cheng, X.; He, B. Affinity Adsorbents for the Vancomycin Group of Antibiotics. *Biotechnol. Appl. Biochem.* **2000**, *31* (1), 15–20. https://doi.org/10.1042/ba19990039.

(82) Zhang, S.; Baker, J.; Pulay, P. A Reliable and Efficient First Principles-Based Method for Predicting PKa Values. 2. Organic Acids. *J. Phys. Chem. A* **2010**, *114* (1), 432–442. https://doi.org/10.1021/jp9067087.

(83) Schüürmann, G.; Cossi, M.; Barone, V.; Tomasi, J. Prediction of the PKa of Carboxylic Acids Using the Ab Initio Continuum-Solvation Model PCM-UAHF. *J. Phys. Chem. A* **1998**, *102* (33), 6706–6712. https://doi.org/10.1021/jp981922f.

(84) Fukuzumi, H.; Saito, T.; Okita, Y.; Isogai, A. Thermal Stabilization of TEMPO-Oxidized Cellulose. *Polym. Degrad. Stab.* **2010**, *95*, 1502–1508. https://doi.org/10.1016/j.polymdegradstab.2010.06.015.

(85) Isogai, A.; Saito, T.; Fukuzumi, H. TEMPO-Oxidized Cellulose Nanofibers. *Nanoscale* **2011**, *3* (1), 71–85. https://doi.org/10.1039/c0nr00583e.

(86) Zhu, L.; Kumar, V.; Banker, G. S. Examination of Aqueous Oxidized Cellulose Dispersions as a Potential Drug Carrier. I. Preparation and Characterization of Oxidized Cellulose-Phenylpropanolamine Complexes. *AAPS PharmSciTech* **2004**, *5* (4), e69–e69. https://doi.org/10.1208/pt050469.

(87) Johnson, J.; Yalkowsky, S. Reformulation of a New Vancomycin Analog: An Example of the Importance of Buffer Species and Strength. *AAPS PharmSciTech* **2006**, *7*, E5.

https://doi.org/10.1208/pt070105.
(88) Shammas, N. K. Coagulation and Flocculation BT - Physicochemical Treatment Processes; Wang, L. K., Hung, Y.-T., Shammas, N. K., Eds.; Humana Press: Totowa, NJ, 2005; pp 103–139. https://doi.org/10.1385/1-59259-820-x:103.
(89) Fijorek, K.; Püsküllüoğlu, M.; Tomaszewska, D.; Tomaszewski, R.; Glinka, A.; Polak, S. Serum Potassium, Sodium and Calcium Levels in Healthy Individuals - Literature Review and Data Analysis. *Folia Med. Cracov.* **2014**, *54* (1), 53–70.
(90) Reynolds, R. M.; Padfield, P. L.; Seckl, J. R. Disorders of Sodium Balance. *BMJ* **2006**, *332* (7543), 702–705. https://doi.org/10.1136/bmj.332.7543.702.
(91) Yee, J. Hypercalcemia; Enna, S. J., Bylund, D. B. B. T. T. C. P. R., Eds.; Elsevier: New York, 2007; pp 1–6. https://doi.org/https://doi.org/10.1016/B978-008055232-3.60633-6.
(92) Sadowy, E. Linezolid Resistance Genes and Genetic Elements Enhancing Their Dissemination in Enterococci and Streptococci. *Plasmid* **2018**, *99*, 89–98. https://doi.org/10.1016/j.plasmid.2018.09.011.
(93) Shallcross, L. J.; Davies, D. S. C. Antibiotic Overuse: A Key Driver of Antimicrobial Resistance. *Br. J. Gen. Pract.* **2014**, *64* (629), 604–605. https://doi.org/10.3399/bjgp14X682561.
(94) Pevere, A.; Guibaud, G.; van Hullebusch, E.; Boughzala, W.; Lens, P. N. L. Effect of Na+ and Ca2+ on the Aggregation Properties of Sieved Anaerobic Granular Sludge. *Colloids Surfaces A Physicochem. Eng. Asp.* **2007**, *306*, 142–149. https://doi.org/10.1016/j.colsurfa.2007.04.033.

ACADEMIC VITA

David T. Kennedy

Education

The Pennsylvania State University, *Schreyer Honors College*
Bachelor of Science in Chemical Engineering
Bachelor of Science in Chemistry

Research and Employment

Honors Thesis Researcher in Sheikhi Lab at Penn State *Fall 2019 - present*

-Applied for and received an Erickson Discovery Grant supporting summer study of the functionalization of crystalline nanocellulose to remove antibiotics from water (focused on vancomycin, daptomycin, and linezolid)
-Characterized materials through DLS, Zeta potential, titration, and FT-IR
-Used absorbance spectroscopy to assess antibiotic precipitation from water following functionalized nanocellulose addition

Medicinal Chemistry Co-op at Vertex Pharmaceuticals *Winter 2020 - Summer 2020*

-Worked full-time in a drug discovery lab at Vertex Pharmaceuticals in Boston to optimize the Larock Indolization for drug synthesis
-Ran small scale reactions to determine conditions to minimize biproduct formation and analyzed results through LCMS, TLC, and NMR
-Applied literature research to design a protocol to determine the factors that affect Larock Indole Synthesis
-Continued contributing to onsite research during the COVID-19 pandemic

Research Intern in Chang Lab at Utah State University *Summer 2019*

-Modified aminoglycosides for antifungal medicinal purposes
-Synthesized and purified a library of 7 amphiphilic kanamycin derivatives including two fluorescent analogs
-Ran reactions, optimized solvents, analyzed NMR, and purified products by column chromatography and recrystallization

Undergraduate Researcher in Curtis Lab at Penn State *Fall 2017- Spring 2019*

-Performed bomb calorimetry and analyzed wastewater heats of combustion
-Executed vacuum infiltration of *Nicotiana benthamiana* for successful Green Fluorescent Protein expression
-Gained four semesters of experience in good laboratory practice in addition to basic skills such as media prep, algae culturing, and plasmid preparation

Extracurriculars

Penn State Club Cross Country Team *Fall 2017 - present*

-2019 executive Board member for the largest club sports team on campus. Actively involved in all club decisions and organizing meets (10+ hours/week)

Honors

Erickson Discovery Grant Winner to support nanocellulose research summer 2020
Academic Excellence Scholarship 2017-2021, CSL Behring Biotechnology Scholarship 2020, Silvestri Scholarship in Chemistry 2020
Named one of Penn State's four Goldwater Fellowship Nominees 2019
Penn State Chemical Engineering Sophomore Scholarship Award 2019
Dean's List Fall 2017-Fall 2020

Other

ACS Spring 2020 National Meeting Poster Presentation: *Surface treatment and temperature effects on luminescence of Ag nanoparticles*
Contributed to two textbook chapters: Hairy Cellulose Nanocrystals: from synthesis to advanced applications in the water volumes 1 and 2 recently accepted
Fluent in French (first language), proficient in Spanish
Proficient in Mathematica, Aspen, Excel, Word, PowerPoint, Visual Basic
NMR, IR, DLS, column chromatography, distillation, recrystallization experience
Interests include running, skiing, hiking, and ice hockey